The Plant Cell, Vol. 26: 1525–1543, April 2014, www.plantcell.org

The ARC1 E3 Ligase Promotes Two Different Self-Pollen Avoidance Traits in *Arabidopsis*[C][W]

Emily Indriolo,[a] Darya Safavian,[a] and Daphne R. Goring[a,b,1]

[a] Department of Cell and Systems Biology, University of Toronto, Toronto M5S 3B2, Canada
[b] Centre for the Analysis of Genome Evolution and Function, University of Toronto, Toronto M5S 3B2, Canada

Flowering plants have evolved various strategies for avoiding self-pollen to drive genetic diversity. These strategies include spatially separated sexual organs (herkogamy), timing differences between male pollen release and female pistil receptivity (dichogamy), and self-pollen rejection. Within the Brassicaceae, these outcrossing systems are the evolutionary default state, and many species display these traits, including *Arabidopsis lyrata*. In contrast to *A. lyrata*, closely related *Arabidopsis thaliana* has lost these self-pollen traits and thus represents an excellent system to test genes for reconstructing these evolutionary traits. We previously demonstrated that the ARC1 E3 ligase is required for self-incompatibility in two diverse Brassicaceae species, *Brassica napus* and *A. lyrata*, and is frequently deleted in self-compatible species, including *A. thaliana*. In this study, we examined *ARC1*'s requirement for reconstituting self-incompatibility in *A. thaliana* and uncovered an important role for *ARC1* in promoting a strong and stable pollen rejection response when expressed with two other *A. lyrata* self-incompatibility factors. Furthermore, we discovered that *ARC1* promoted an approach herkogamous phenotype in *A. thaliana* flowers. Thus, *ARC1*'s expression resulted in two different *A. lyrata* traits for self-pollen avoidance and highlights the key role that ARC1 plays in the evolution and retention of outcrossing systems.

INTRODUCTION

In flowering plants, sexual reproduction can involve complex interactions between male pollen grains and the female pistil for increasing genetic diversity. Flowers have evolved multiple strategies to ensure outcrossing, and these start at the moment that pollen lands on the stigma at the top of the pistil. One strategy in bisexual flowers is the spatial separation of the male and female organs (herkogamy) with the most common arrangement having the stigma positioned above the pollen producing anthers (referred to as approach herkogamy) (Webb and Lloyd, 1986; Barrett, 2003; Charlesworth, 2006). Another is to have the temporal separation of the male and female functions where the timing of pollen release by the anthers differs from stigma receptivity for pollination (dichogamy) (Lloyd and Webb, 1986; Barrett, 2003; Charlesworth, 2006). In addition to these morphological and temporal characteristics, flowering plants may have a self-incompatibility system where self-pollen is recognized and rejected (reviewed in Iwano and Takayama, 2012).

Within the mustard family (Brassicaceae), *Arabidopsis lyrata* can display all three of these traits: self-incompatibility, approach herkogamy, and a type of dichogamy where stigma receptivity occurs prior to pollen release (Indriolo et al., 2012; Luo and Widmer, 2013). Another species, *Arabidopsis thaliana* is typically a selfing plant and has nonherkogamous flowers; however, two natural *A. thaliana* accessions, BRA and SIM, from high altitudes were recently reported to display approach herkogamy (Luo and Widmer, 2013). Two studies have investigated the morphological characteristics associated with the selfing syndrome in *Capsella rubella*, and quantitative trait loci (QTL) were mapped using an F2 population from a selfing *C. rubella* crossed with an outcrossing *Capsella grandiflora* (Sicard et al., 2011; Slotte et al., 2012). Among the characteristics measured was the degree of spatial separation between the anthers and stigma, and several QTLs were identified that influenced this trait, though no candidate genes were reported (Sicard et al., 2011; Slotte et al., 2012).

In the Brassicaceae, the self-incompatibility signaling pathway to reject self-pollen has been well-characterized in *Brassica* species (*Brassica oleracea*, *Brassica napus*, and *Brassica rapa*). The signaling pathway is initiated with the landing of a self-pollen grain on a stigmatic papilla, and the pollen *S*-locus Cysteine Rich/*S*-locus Protein 11 (SCR/SP11) ligand is detected by the allele-specific *S* Receptor Kinase (SRK) in the stigmatic papilla (Kachroo et al., 2001; Takayama et al., 2001; Shimosato et al., 2007). After binding, SRK activates a signaling pathway in the stigmatic papilla that rapidly rejects pollen by blocking pollen hydration or pollen tube penetration into the stigmatic surface (reviewed in Chapman and Goring, 2010; Ivanov et al., 2010). The *SCR/SP11* and *SRK* genes are highly polymorphic, and alleles have been identified in other species, including *A. lyrata* (Kusaba et al., 2001; Schierup et al., 2001, 2006; Prigoda et al., 2005; Mable and Adam, 2007) and *C. grandiflora* (Paetsch et al., 2006; Boggs et al., 2009b; Guo et al., 2009). Downstream of SRK in the self-incompatibility pathway, there are two positive regulators that have been shown to interact with SRK, *M* locus Protein Kinase (MLPK) and the E3 ubiquitin ligase, ARM-Repeat Containing1 (ARC1) (Gu et al., 1998; Kakita et al., 2007a, 2007b). *B. rapa* MLPK is a receptor-like

[1] Address correspondence to d.goring@utoronto.ca.
The author responsible for distribution of materials integral to the findings presented in this article in accordance with the policy described in the Instructions for Authors (www.plantcell.org) is: Daphne R. Goring (d.goring@utoronto.ca).
[C] Some figures in this article are displayed in color online but in black and white in the print edition.
[W] Online version contains Web-only data.
www.plantcell.org/cgi/doi/10.1105/tpc.114.122879

cytoplasmic kinase localized to the plasma membrane with SRK and is required for the self-incompatibility response, as *mlpk* mutants were unable to reject self-pollen (Murase et al., 2004; Kakita et al., 2007b).

ARC1 is a Plant U-box (PUB) E3 ubiquitin ligase that is required for the self-incompatibility response in both *B. napus* and *A. lyrata* (Stone et al., 1999, 2003; Indriolo et al., 2012). U-box E3 ligases function as scaffolds for ubiquitination by recruiting E2 conjugating enzymes to the U-box domain and binding target substrate proteins through other domains present in the protein (Zhang et al., 2005; Xu et al., 2008; Nordquist et al., 2010). Exo70A1 was identified as a target of ARC1 and is ubiquitinated by ARC1 (Samuel et al., 2009). Exo70A1 is a subunit of the exocyst complex that tethers secretory vesicles to the plasma membrane for secretion (reviewed in Zhang et al., 2010; Heider and Munson, 2012). During the basal pollen recognition response, Exo70A1, as part of the exocyst complex, is proposed to direct secretory vesicles to the papillar plasma membrane directly under the pollen contact site to deliver cargo required for pollen hydration and pollen tube penetration into the stigmatic surface (Samuel et al., 2009; Safavian and Goring, 2013). ARC1 is predicted to promote self-pollen rejection in the self-incompatibility pathway by inhibiting Exo70A1 and by blocking/overriding the delivery of secretory vesicles in the basal pollen recognition response (Samuel et al., 2009; Safavian and Goring, 2013). Supporting this model, vesicle-like structures are present at the stigmatic papillar plasma membrane in compatible *A. thaliana* and *A. lyrata* pollinations while absent from self-incompatible *A. lyrata* pollinations (Safavian and Goring, 2013).

A. thaliana is a self-compatible species, and while some *A. thaliana* ecotypes still carry an intact *SCR* or *SRK* gene, the majority have been shown to carry nonfunctional *SCR* and *SRK* genes; this loss was hypothesized to be a key part of the transition to selfing from self-incompatibility (Kusaba et al., 2001; Bechsgaard et al., 2006; Tang et al., 2007; Shimizu et al., 2008; Boggs et al., 2009a; Tsuchimatsu et al., 2010; Guo et al., 2011). Previous work into the reconstruction of the self-incompatibility signaling pathway in *A. thaliana* with functional *SCR* and *SRK* genes has shown mixed results with considerable variability in the strength and stability of the self-incompatibility responses (Nasrallah et al., 2004; Boggs et al., 2009a, 2009b; Tsuchimatsu et al., 2010). Recently, we have shown that *ARC1* is necessary for self-pollen rejection in the naturally self-incompatible *A. lyrata* species; interestingly, *ARC1* is frequently deleted in self-compatible species, including *A. thaliana* (Indriolo et al., 2012). These observations support that the self-incompatibility pathway is highly conserved across the Brassicaceae and that the loss of a functional *ARC1* gene may be associated with the transition from self-incompatibility to self-compatibility (Indriolo et al., 2012). Therefore, in this study, we investigated the role of *ARC1* in reconstructing the self-incompatibility response in *A. thaliana*.

RESULTS

Reconstitution of the *SCRb-SRKb-ARC1* Signaling Pathway in *A. thaliana* Plants

Our recent research has shown that ARC1 is required for self-pollen rejection in self-incompatible *A. lyrata* and that there was a wide-spread deletion of *ARC1* across 357 *A. thaliana* ecotypes tested (Indriolo et al., 2012). Thus, we set out to test what effect the addition of *ARC1* would have on reconstructing the self-incompatibility response in *A. thaliana*. Previous research into the reconstruction of the self-incompatibility signaling pathway in *A. thaliana* using the *SCRb-SRKb* genes has shown that some ecotypes remained compatible; other ecotypes displayed self-pollen rejection, but with variability in the timing and strength of the self-incompatibility response (Nasrallah et al., 2004; Boggs et al., 2009a). Based on these previous reports, two ecotypes were chosen to test ARC1's putative role: *A. thaliana* ecotype Columbia-0 (Col-0), which remained self-compatible, and *A. thaliana* ecotype Sha, which displayed self-incompatibility with the transformation of the *SCRb-SRKb* genes (Nasrallah et al., 2004; Boggs et al., 2009a). Both ecotypes have endogenous pseudogenes for *SCRa* and *SRKa*, and *ARC1* has been deleted (Kusaba et al., 2001; Boggs et al., 2009a; Kitashiba et al., 2011; Indriolo et al., 2012).

To examine the SCR-SRK signaling pathway, in the presence and absence of ARC1, we used the previously tested p548 vector carrying the *A. lyrata SRKb* and *SCRb* genes (Nasrallah et al., 2004; Boggs et al., 2009a). The *SCRb-SRKb* + *ARC1* transgenic Col-0 and Sha plants were generated by cotransforming the ARC1 transformation vector with p548. Twenty independent transgenic lines were generated for each combination of transgenes, and these lines were selected at random with no preselection bias (Tables 1 and 2). To study the conservation of the function of ARC1 between *A. lyrata* and *B. napus*, we examined both *A. lyrata* ARC1 (Al-*ARC1*) and *B. napus* ARC1 (Bn-*ARC1*) orthologs in combination with *SCRb-SRKb*. The rationale for this was that Al-ARC1 and Bn-ARC1 are more divergent in their amino acid sequences compared with other orthologous pairs in this family (Indriolo et al., 2012). The Al-ARC1 protein is 701 amino acids in length versus the shorter Bn-ARC1 at 661 amino acids, and the two proteins share 65% amino acid sequence identity (Supplemental Figure 1). In comparison, the closest ARC1 paralogs, *A. lyrata* PUB17 and *B. rapa* PUB17 (two copies; Indriolo et al., 2012), are highly conserved with 86% amino acid sequence identity and similar in length (722 amino acids for *A. lyrata*; 704 and 719 amino acids for *B. rapa*).

Self-Incompatible Plants Are Generated with the Expression of *SCRb-SRKb-ARC1* in the *A. thaliana* Col-0 Ecotype

For each transgene combination, 20 independent T0 plants were characterized for their self-incompatibility phenotypes by the use of aniline blue stain for pollen germination and pollen tube penetration into the pistil. The initial phenotypes were scored based on whether the stigmas displayed a self-compatible, a moderate self-incompatible, or a strong self-incompatible phenotype (Table 1, Figure 1). Pistils were manually pollinated with self-pollen at the stage where the flowers are fully open and pollen is released (Smyth et al., 1990). Plants were defined as self-compatible if self-pollen grains were accepted similarly to self-pollinated wild-type Col-0 pistils (Figures 1A and 1B). Plants characterized as strongly self-incompatible rejected self-pollen with little to no pollen grains adhering and pollen tubes rarely penetrated (<10 pollen tubes/pistil). Plants that were characterized

Table 1. Self-Incompatibility Phenotypes of Transgenic *A. thaliana* in the Col-0 Ecotype

Transgenes	Self-Incompatible		Self-Compatible	Total No. T0 Plants Tested
	Strong	Moderate		
SCRb-SRKb	0	0	20	20
SCRb-SRKb + Al-*ARC1*	5	11	4	20
SCRb-SRKb + Bn-*ARC1*	7	6	7	20

Phenotypes were assessed by pollinating emasculated late stage 13 pistils (open flowers) with self-pollen for 2 h, followed by aniline blue staining of the pollinated pistils to view pollen tube growth. The T0 plants were scored as "strong self-incompatible" if <10 pollen tubes/pistil were observed or "moderate self-incompatible" if >10 pollen tubes/pistil were observed and there was a clear reduction in the number of pollen tubes relative to the self-compatible controls (n = 3 pistils/T0 plant).

as having moderately self-incompatible stigmas displayed more than 10 pollen tubes/pistil, but there was a clear reduction in the number of pollen tubes relative to the self-compatible controls. Representative differential interference contrast and aniline blue–stained pistils for these different categories are shown in Figure 1.

The results of surveying 20 randomly selected independent transgenic T0 plants for each transgene combination were quite clear. As previously described (Nasrallah et al., 2004; Boggs et al., 2009a), *A. thaliana* Col-0 plants with the *SCRb-SRKb* genes alone were fully self-compatible (Table 1, Figures 1C and 1D). However, the transformation of either Al-*ARC1* or Bn-*ARC1* with the *SCRb-SRKb* vector resulted in the generation of transgenic *A. thaliana* Col-0 plants that were self-incompatible (Table 1). Of the 20 transgenic T0 Col-0 *SCRb-SRKb* + Al-*ARC1* plants, five displayed strong self-incompatibility phenotypes (Figures 1E and 1F) and 11 had moderate self-incompatibility responses (Figures 1G and 1H). The observed self-incompatibility phenotypes were not a result of other fertility issues as control reciprocal crosses with wild-type Col-0 produced fully compatible pollinations (Supplemental Figure 2). Similar to the *SCRb-SCRKb* + Al-*ARC1* plants, of the 20 transgenic T0 Col-0 *SCRb-SRKb* + Bn-*ARC1* plants, seven exhibited strong self-incompatibility phenotypes (Figures 1K and 1L) and six displayed moderate self-incompatibility responses (Figures 1M and 1N). Finally, both genotypes (Al-*ARC1* and Bn-*ARC1*) contained several transgenic T0 plants that displayed a fully self-compatible phenotype when examined with aniline blue staining (Figures 1I, 1J, 1O, and 1P). The fact that out of 20 randomly selected lines, 16 *SCRb-SRKb* + Al-*ARC1* plants and 13 *SCRb-SRKb* + Bn-*ARC1* plants showed some level of self-pollen rejection indicates that there is a function for ARC1 in the reconstructed self-incompatibility pathway in *A. thaliana* in the Col-0 ecotype.

Expression of *SCRb-SRKb-ARC1* in the *A. thaliana* Sha Ecotype Results in a Stronger Self-Incompatibility Phenotype

A. thaliana Sha was previously reported to become self-incompatible with the expression of *SCRb-SRKb*, but this phenotype was leaky as the plants still produced some seeds (Boggs et al., 2009a). Thus, we were interested to see if the addition of *ARC1* with *SCRb-SRKb* results in an even stronger self-incompatibility phenotype. Similar to the Col-0 transgenic plants, 20 independent T0 plants were selected for each transgene combination without any preselection bias (17 T0 plants were examined for the Sha *SCRb-SRKb* genotype). The T0 plants were again manually pollinated with self-pollen and characterized by aniline blue stain and scored for the distribution of strong self-incompatible, moderate self-incompatible, or self-compatible phenotypes (Table 2). Representative images of these phenotypes are shown in Figure 2.

Three of the *A. thaliana* Sha *SCRb-SRKb* T0 plants did show a self-incompatibility phenotype though the phenotype was moderate (Table 2, Figures 2C and 2D). This is unlike the observations in Col-0 where all of the *A. thaliana* Col-0 *SCRb-SRKb* T0 plants remained self-compatible (Table 1) but is consistent with *A. thaliana* Sha *SCRb-SRKb* lines previously observed to have a self-incompatibility phenotype (Boggs et al., 2009a). When all three genes were expressed, a strong self-incompatibility phenotype was observed. Compared with the results seen for the *A. thaliana* Col-0 transgenic plants (Table 1), the number of *A. thaliana* Sha transgenic T0 plants displaying the strong phenotype was higher (Table 2). This was observed in 10 out of 20 transgenic *A. thaliana* Sha *SCRb-SRKb* + Al-*ARC1* T0 plants (Figures 2G and 2H), and 14 out of 20 transgenic *A. thaliana* Sha *SCRb-SRKb* + Bn-*ARC1* T0 plants (Figures 2M and 2N). Control reciprocal crosses with wild-type Sha produced fully compatible pollinations, indicating that the observed phenotypes were due to self-incompatibility (Supplemental Figure 2). Also, fewer *A. thaliana* Sha T0 plants displayed a moderate self-incompatibility phenotype (Table 2) with six T0 plants for *SCRb-SRKb* + Al-*ARC1* (Figures 2I and 1J) and five T0 plant for *SCRb-SRKb* + Bn-*ARC1* (Figures 2O and 2P). Finally, there were few *A. thaliana* Sha T0 plants that remained self-compatible (Table 2) with four T0 plants for *SCRb-SRKb* + Al-*ARC1* (Figures 2K and 2L) and one T0 plant for *SCRb-SRKb* + Bn-*ARC1* (Figures 2Q and 2R) displaying a phenotype comparable to self-pollinated wild-type *A. thaliana* Sha pistils (Figures 2A and 2B). Thus, a more robust self-incompatibility phenotype is observed with the addition of *ARC1* with *SCRb-SRKb* in the *A. thaliana* Sha ecotype.

Table 2. Self-Incompatibility Phenotypes of Transgenic *A. thaliana* in the Sha Ecotype

Transgenes	Self-Incompatible		Self-Compatible	Total No. T0 Plants Tested
	Strong	Moderate		
SCRb-SRKb	0	3	14	17
SCRb-SRKb + Al-*ARC1*	10	6	4	20
SCRb-SRKb + Bn-*ARC1*	14	5	1	20

Phenotypes were assessed by pollinating emasculated late stage 13 pistils (open flowers) with self-pollen for 2 h, followed by aniline blue staining of the pollinated pistils to view pollen tube growth. The T0 plants were scored as "strong self-incompatible" if <10 pollen tubes/pistil were observed or "moderate self-incompatible" if >10 pollen tubes/pistil were observed and there was a clear reduction in the number of pollen tubes relative to the self-compatible controls (n = 3 pistils/T0 plant).

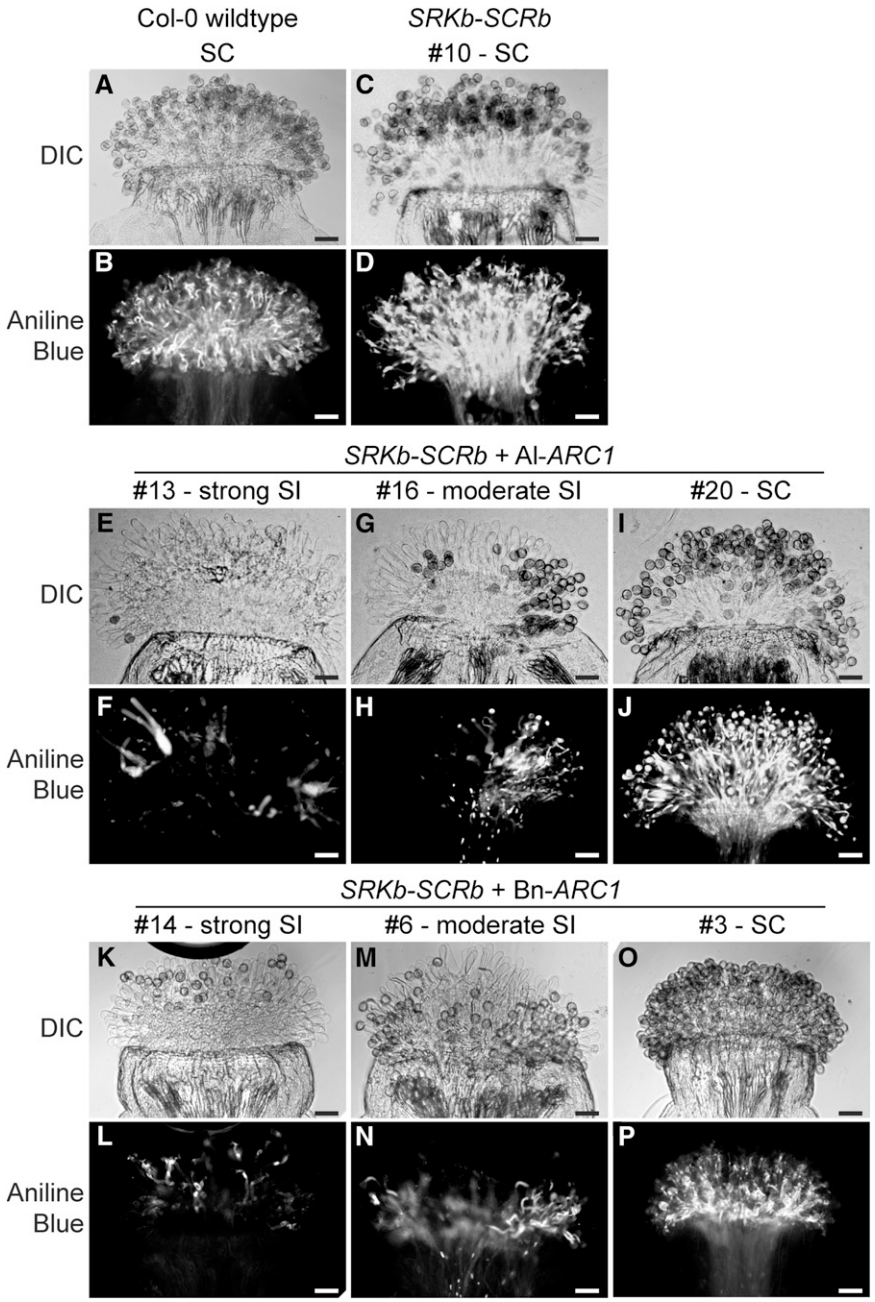

Figure 1. Pollen Grain Attachment and Pollen Tube Growth in Transgenic *A. thaliana* Col-0 Plants.

(A) and **(B)** Wild-type *A. thaliana* Col-0 stigma pollinated with self-compatible pollen.
(C) and **(D)** *A. thaliana* Col-0 *SCRb-SRKb* plant #10 self-pollinated.
(E) to **(J)** *A. thaliana* Col-0 *SCRb-SRKb* + Al-*ARC1* plants #13, 16, and 20 self-pollinated.
(K) to **(P)** *A. thaliana* Col-0 *SCRb-SRKb* + Bn-*ARC1* plants #14, 6, and 3 self-pollinated.
Differential interference contrast (DIC) and aniline blue–stained images are shown for each pollinated stigma. SC, self-compatible; SI, self-incompatible. Bars = 50 μm.

Expression of *SCRb-SRKb-ARC1* in the *A. thaliana* Col-0 and Sha Ecotypes Leads to an Approach Herkogamous Phenotype

During the analysis of the *A. thaliana SCRb-SRKb-ARC1* transgenic plants, we observed a second and distinct phenotype in these transgenic plants; the flowers had an altered morphology resulting in approach herkogamy where the stigmas were positioned above the anthers (Webb and Lloyd, 1986). Approach herkogamy is a trait found in *A. lyrata* (Luo and Widmer, 2013) and an example is shown for *A. lyrata* ssp *petraea*, which we have previously worked

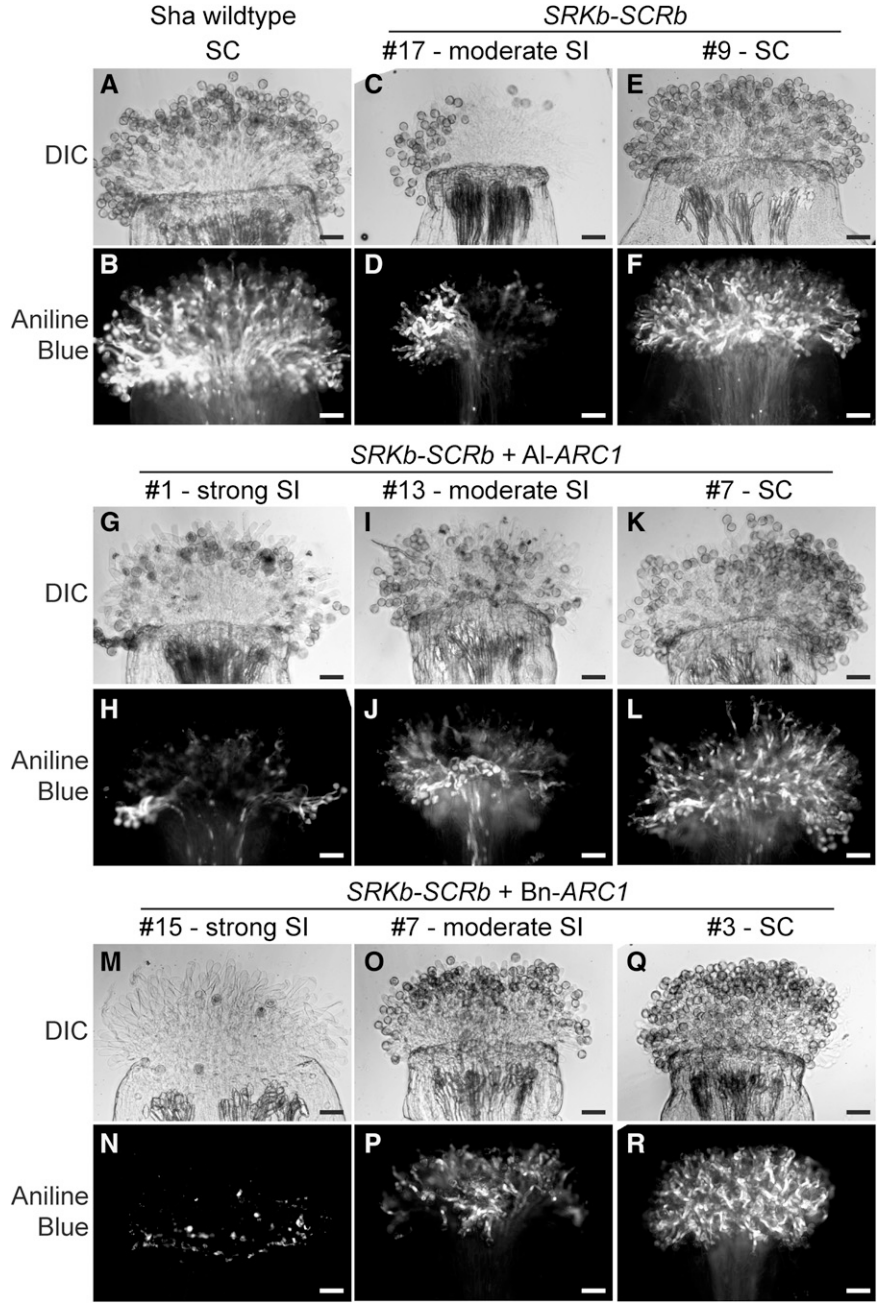

Figure 2. Pollen Grain Attachment and Pollen Tube Growth in Transgenic *A. thaliana* Sha Plants.

(A) and **(B)** Wild-type *A. thaliana* Sha stigma pollinated with self-compatible pollen.
(C) to **(F)** *A. thaliana* Sha *SCRb-SRKb* plants #17 and 9 self-pollinated.
(G) to **(L)** *A. thaliana* Sha *SCRb-SRKb* + Al-*ARC1* plants #1, 13, and 7 self-pollinated.
(M) to **(R)** *A. thaliana* Sha *SCRb-SRKb* + Bn-*ARC1* plants #15, 7, and 3 self-pollinated.
Differential interference contrast (DIC) and aniline blue–stained images are shown for each pollinated stigma. SC, self-compatible; SI, self-incompatible. Bars = 50 μm.

with (Figure 3A; Indriolo et al., 2012). This trait is not found in the vast majority of *A. thaliana* ecotypes (including Col-0 and Sha; Figures 3B and 3F) but has been recently reported in two natural accessions, BRA and SIM (Luo and Widmer, 2013). The approach herkogamous phenotype was not detected in the *A. thaliana* Col-0 plants expressing only *SCRb-SRKb* (Table 3, Figures 3C and 3G), while transgenic lines that expressed all three *SCRb-SRKb-ARC1* genes with either Al-*ARC1* or Bn-*ARC1* displayed this phenotype (Table 3, Figures 3D and 3E). Interestingly, this trait was observed in all 20 transgenic *SCRb-SRKb-ARC1* lines in the Col-0 ecotype (Table 3).

Similarly, the transgenic *A. thaliana* Sha plants expressing only *SCRb-SRKb* did not display approach herkogamous flowers (Table 3, Figure 3G). In contrast, all 20 transgenic *A. thaliana* Sha *SCRb-SRKb-ARC1* lines with either Al-*ARC1* or Bn-*ARC1* produced approach herkogamous flowers (Table 3, Figures 3H and 3I).

To further examine the approach herkogamy trait, the degree of the physical separation between anthers and stigmas (SAS) was measured in flowers from representative transgenic lines as previously described by Luo and Widmer (2013). This analysis examined the physical distance between the stigma and the anthers by comparing the stigma height to the anther height (Figure 3J). A positive SAS value indicates approach herkogamy and was seen in the transgenic lines expressing *SCRb-SRKb-ARC1* in both the Col-0 and Sha ecotypes (Figure 3J). This phenotype was due to increases in pistil length, and the stamen length was not affected (Supplemental Figure 3). In contrast, Col-0 and Sha wild-type flowers and the transgenic lines expressing only *SCRb-SRKb* showed negative values indicative of a reverse herkogamous phenotype (Figure 3J). As a control, two transgenic Col-0 plants expressing only Al-*ARC1* were examined and were found to have either a neutral or reverse herkogamous phenotype (Figure 3J). The SAS measurements for these Al-*ARC1* lines were not significantly different from the other reverse herkogamous flowers ($P < 0.05$). Therefore, the expression of *ARC1* along with *SCRb-SRKb* is required to induce the approach herkogamous phenotype.

Seed Set Is Strongly Reduced in the Self-Incompatible *SCRb-SRKb-ARC1 A. thaliana* Col-0 and Sha Lines

As the purpose of self-incompatibility is to block self-pollen germination and pollen tube growth so that fertilization is prevented, we examined the ability of the strong self-incompatible *SCRb-SRKb-ARC1* transgenic plants to produce seeds. When these plants were allowed to set seed naturally, the reduced self-pollination in the self-incompatible lines was associated with shorter silique lengths, indicative of reduced seed production. Representative photographs of branches with siliques are shown in Figure 4. Both wild-type *A. thaliana* Col-0 and Sha are fully self-compatible and displayed regular silique sizes (Figures 4A and 4E). Similarly, the self-compatible *A. thaliana* Col-0 *SCRb-SRKb* plants and *A. thaliana* Sha *SCRb-SRKb* plants displayed fully developed siliques (Figures 4B and 4F). Some reduction in silique size was observed for the *A. thaliana* Sha *SCRb-SRKb* plants displaying a moderate self-incompatibility response (Figure 4G). However, the *A. thaliana* Col-0 and Sha transgenic plants expressing *SCRb-SRKb* with either Al-*ARC1* or Bn-*ARC1* showed much smaller siliques (Figures 4C, 4D, 4H, and 4I).

The small siliques are indicative of a reduced seed production; however, the approach herkogamous phenotype displayed by the *SCRb-SRKb-ARC1* could influence seed set in these plants. When mature pollen grains are released from the anthers, the pollen grain may end up deposited on the side of the pistil rather than on top of the stigma, preventing self-pollination and resulting in reduced seed set. To look at the contributions of the self-incompatibility trait, manual self-pollinations were performed at the stage where the flowers are fully open, and the siliques were allowed to fully develop. Mature siliques were dissected and the total number of seeds per silique was scored (Figure 5). The siliques of wild-type *A. thaliana* Col-0 plants contained an average of 50.3 seeds/silique when manually pollinated, and the siliques from the three self-compatible *A. thaliana* Col-0 *SCRb-SRKb* plants showed a similar range with averages of 51.8, 53.2, and 49.1 seeds/silique (Figure 5A). Therefore, the *A. thaliana* Col-0 *SCRb-SRKb* lines were wild-type in regards to their ability to accept self-pollen and set seeds. In contrast, when the three strongest self-incompatible *A. thaliana* Col-0 transgenic lines expressing *SCRb-SRKb* with either Al-*ARC1* or Bn-*ARC1* were pollinated, all lines showed significant reductions in the number of seeds/silique compared with wild-type *A. thaliana* Col-0 and the Col-0 *SCRb-SRKb* lines. The lowest values were observed for *A. thaliana* Col-0 *SCRb-SRKb* + Al-*ARC1* line 18 with an average of 9.0 seeds/silique and *A. thaliana* Col-0 *SCRb-SRKb* + Bn-*ARC1* line 14 with an average of 5.6 seeds/silique (Figure 5A). Thus, the addition of either Al-*ARC1* or Bn-*ARC1* with *SCRb-SRKb* in *A. thaliana* Col-0 produced a significant reduction in seeds due to self-pollen rejection.

Similarly, manual pollinations for seed set were performed on the strongest three lines for the two different *SCRb-SRKb* + *ARC1* transgene combinations in the *A. thaliana* Sha ecotype. In addition, for the *A. thaliana* Sha *SCRb-SRKb* plants, the three moderately self-incompatible lines and three self-compatible lines were analyzed (Figure 5B). The manually pollinated wild-type *A. thaliana* Sha plants showed an average number of 53.5 seeds/silique and the self-compatible *A. thaliana* Sha *SCRb-SRKb* plants displayed similar ranges with 46.2, 50.4, and 51.1 seeds/silique. Interestingly, lower seed set values were observed for the three moderately self-incompatible *A. thaliana* Sha *SCRb-SRKb* lines with values of 16.6, 27.5, and 21.4 seeds/silique. These lines all showed a significant reduction when compared with the wild-type Sha and the three self-compatible *A. thaliana* Sha *SCRb-SRKb* lines (Figure 5B). When either Al-*ARC1* or Bn-*ARC1* was expressed with *SCRb-SRKb* in the Sha ecotype, the seed set reduction was even more substantial, with almost no seeds set in the lines surveyed. The *A. thaliana* Sha *SCRb-SRKb* + Al-*ARC1* lines displayed averages of 1.2 (line 1), 1.3 (line 2), and 3.1 (line 5) seeds/silique, and 60% of the siliques in the strongest lines (1 and 2) had no seeds. Two of the *A. thaliana* Sha *SCRb-SRKb* + Bn-*ARC1* lines displayed very low seed set with averages of 3.5 (line 1) and 0.7 (line 10) seeds/silique, and 80% of the siliques in the strongest line (line 10) did not contain any seeds. Thus, these five lines showed significant reductions in the number of seeds/silique when compared with wild-type *A. thaliana* Sha and the six *A. thaliana* Col-0 *SCRb-SRKb* lines (Figure 5B). The *A. thaliana* Sha *SCRb-SRKb* + Bn-*ARC1* line 15 showed slightly higher levels of seed set with 13 seeds/silique and was significantly different to wild-type *A. thaliana* Sha and the three self-compatible *A. thaliana* Sha *SCRb-SRKb* lines (Figure 5B). Thus, the addition of either Al-*ARC1* or Bn-*ARC1* with *SCRb* and *SRKb* in the *A. thaliana* Sha ecotype leads to very strong rejection of self-pollen, resulting in almost no seeds produced.

The Addition of the *ARC1* Transgene Is Not Correlated with Higher Expression Levels of *SCRb* and *SRKb*

With our observations that the addition of the *ARC1* transgene resulted in much stronger self-incompatibility responses, we

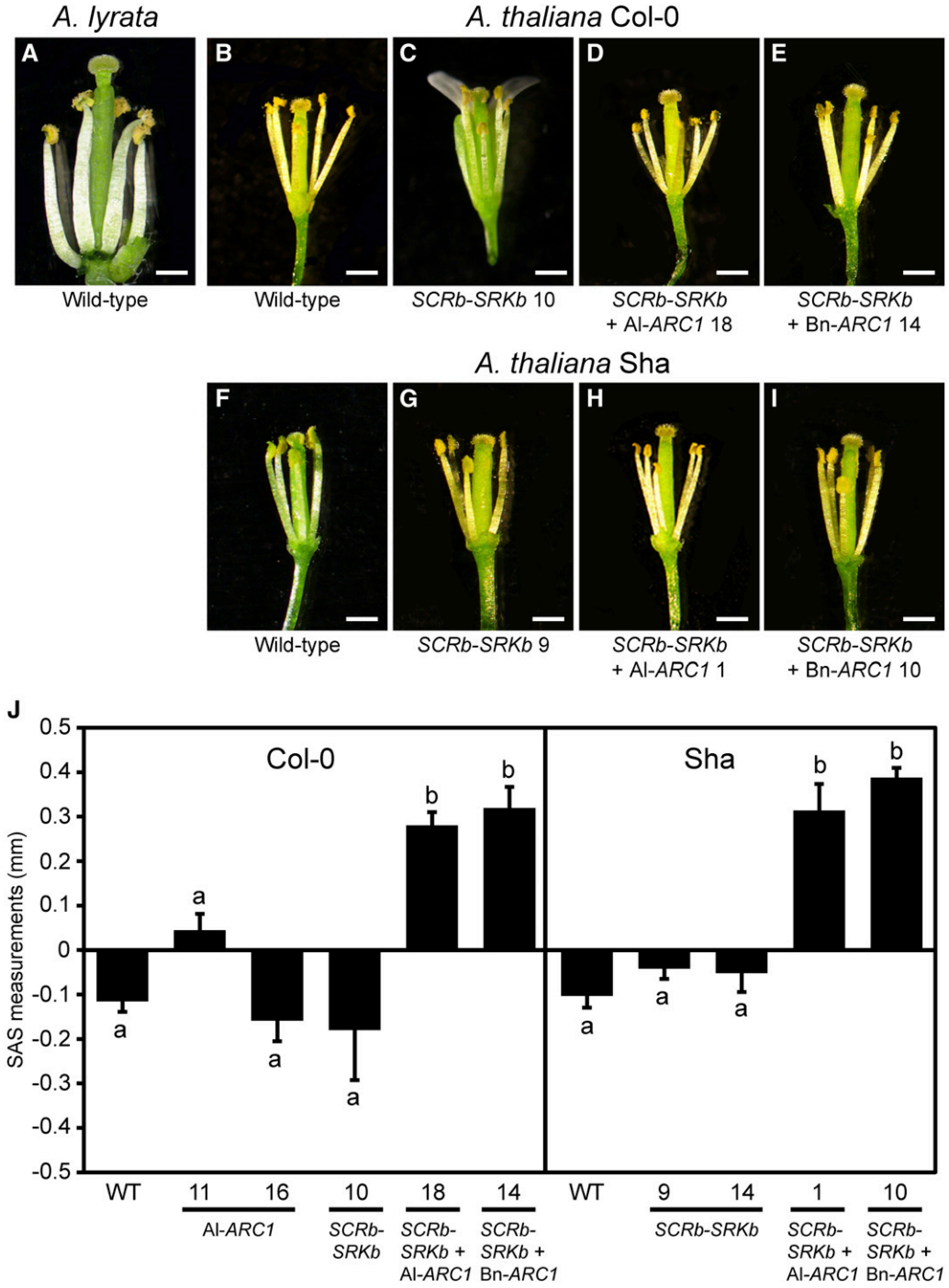

Figure 3. Approach Herkogamous Phenotypes in Transgenic *A. thaliana* Col-0 and Sha *SCRb-SRKb-ARC1* Plants at Anthesis.

(A), **(B)**, and **(F)** Flowers from wild-type *A. lyrata*, *A. thaliana* Col-0, and *A. thaliana* Sha plants.
(C) to **(E)** Flowers from *A. thaliana* Col-0 transgenic plants: *SCRb-SRKb* #10, *SCRb-SRKb* + Al-*ARC1* #18, and *SCRb-SRKb* + Bn-*ARC1* #14.
(G) to **(I)** Flowers from *A. thaliana* Sha transgenic plants: *SCRb-SRKb* #9, *SCRb-SRKb* + Al-*ARC1* #1, and *SCRb-SRKb* + Bn-*ARC1* #10. Bars = 500 μm.
(J) Mean SAS measurements (Luo and Widmer, 2013) for transgenic *A. thaliana* Col-0 and Sha flowers. $n = 9$ flowers per sample. Error bars indicate SE. The different letters represent means that are significantly different at $P < 0.05$ (one-way ANOVA with Tukey-HSD post-hoc tests).
[See online article for color version of this figure.]

Table 3. Herkogamous Phenotypes of Transgenic *A. thaliana* Plants

Species and Ecotype	Transgenes	Floral Phenotype (No. of T0 Plants)	
		Nonherkogamous	Approach Herkogamous
A. thaliana Col-0	–	20	0
	SCRb-SRKb	20	0
	SCRb-SRKb + Al-*ARC1*	0	20
	SCRb-SRKb + Bn-*ARC1*	0	20
A. thaliana Sha	–	20	0
	SCRb-SRKb	17	0
	SCRb-SRKb + Al-*ARC1*	0	20
	SCRb-SRKb + Bn-*ARC1*	0	20
A. lyrata	–	0	10

The position of the stigma relative to the anthers was assessed for freshly opened flowers. A nonherkogamous flower has the stigma and anthers positioned at the same height, while an approach herkogamous flower has the stigma positioned above the anthers.

investigated whether this effect was due to changes in transgene expression levels. We would predict that there would be no correlation between the presence of *ARC1* and the relative *SCRb-SRKb* mRNA levels if the ARC1 protein is acting in the self-incompatibility pathway rather than merely influencing *SCRb-SRKb* gene expression. The relative expression levels of *SCRb* in anthers, and *SRKb* and Al-*ARC1* or Bn-*ARC1* in pistils were quantified using quantitative RT-PCR (qRT-PCR) for both transgenic *A. thaliana* Col-0 and Sha plants (Figure 6). The wild-type expression levels of *ARC1* and *SRK1* in *A. lyrata* stigmas were measured for comparison to the transgenic *A. thaliana* plants. The *SCRb* expression levels in anthers were consistent across most of the lines and in the 1- to 2-fold range, relative to the controls (Figure 6A). A few lines showed increased *SCRb* expression in the 4- to 8-fold range, but the higher relative expression levels were not associated with the presence of the *ARC1* transgene (e.g., *A. thaliana* Sha *SCRb-SRKb* line 14; Figure 6A). The relative *SRKb* expression levels were more variable across the lines (2- to 8-fold range), with a number of lines showing *SRKb* expression levels similar to the 2.8-fold of Al-*SRK1* in *A. lyrata* stigmas (Figure 6B). Again, there was no clear correlation between higher *SRKb* expression levels and the presence of the *ARC1* transgene. For example, two of the self-incompatible *A. thaliana* transgenic Sha lines that showed strong reductions in seed set, *SCRb-SRKb* + Al-*ARC1* line 5 and *SCRb-SRKb* + Bn-*ARC1* line 10, had lower relative *SRKb* expression levels of 2- and 3.2-fold, respectively. In contrast, the fully fertile *A. thaliana SCRb-SRKb* transgenic lines, Col-0 line 8 and Sha line 4, had higher relative *SRKb* expression levels of 6- and 4.8-fold, respectively (Figure 6B). Lastly, the relative *SRKb* expression levels in the three moderately self-incompatible *A. thaliana* Sha *SCRb-SRKb* lines (6.4-, 2.0-, and 1.3-fold) were in a comparable range to the three strongly self-incompatible *A. thaliana* Sha *SCRb-SRKb* Al-*ARC1* lines (6.6-, 2.6-, and 2.0-fold) (Figure 6B). Thus, the presence of the *ARC1* transgene did not result in higher *SCRb* and *SRKb* transcript levels, so the additive effect of ARC1 on *A. thaliana* self-incompatibility is due to the function of the ARC1 protein.

Additionally, we examined the expression level trends between self-compatible and self-incompatible *SCRb-SRKb-ARC1* lines. The relative levels of either Al-*ARC*1 or Bn-*ARC1* expression in several of the transgenic lines were in the 4- to 7-fold range, which was similar to the 5-fold Al-*ARC1* expression levels measured for *A. lyrata* stigmas (Figure 6C). Based on expression levels, the main observation is that for each ecotype, either *SRKb* or *ARC1* expression levels were lower in the self-compatible *SCRb-SCRb+ARC1* line versus the self-incompatible *SCRb-SCRb+ARC1* lines. That is, the self-compatible *A. thaliana* Col-0 *SCRb-SRKb* + Al-*ARC1* line 20 had the lowest *ARC1* expression levels (3.6-fold) for the Col-0 lines (Figure 6C), and the self-compatible *A. thaliana* Sha *SCRb-SRKb* + Bn-*ARC1* line 3 had the lowest *SRKb* expression levels (1-fold) for the Sha lines (Figure 6B). Therefore, *SRKb* and *ARC1* expression needs to be above a certain level to exhibit a self-incompatible phenotype.

Secretory Activity Is Disrupted following Self-Pollination in the Self-Incompatible *A. thaliana* Transgenic Lines

With the reconstituted *SCRb-SRKb-ARC1* signaling pathway producing a self-incompatibility phenotype in the transgenic *A. thaliana* plants, we investigated the cellular responses at the ultrastructural level using transmission electron microscopy (TEM). Following compatible pollinations in *A. thaliana* Col-0 and *A. lyrata* ssp *petraea*, we previously observed two main features in TEM images at 10 min postpollination. First, vesicle-like structures were observed fusing to the stigmatic papillar plasma membrane under the pollen contact site. Second, the vacuole repositioned itself toward the pollen-stigma interface (perhaps to facilitate pollen hydration), resulting in a very thin layer in the cytoplasm in the stigmatic papilla (Figures 7A and 7B; Safavian and Goring, 2013). This was observed in *A. thaliana* Sha at 10 min postcompatible pollination (Figures 7C and 7D). In response to self-incompatible pollen in *A. lyrata* ssp *petraea*, both of these features were absent, and vesicles were redirected to the vacuole for degradation, likely through autophagic bodies (Figures 7E and 7F; Safavian and Goring, 2013). The example shown in Figure 7E is reminiscent of autophagic bodies that have engulfed cytoplasm with ribosomes (Hamasaki et al., 2005; Nakatogawa and Ohsumi, 2008). Therefore, there are clear cellular changes at the ultrastructural level that differentiated compatible and self-incompatible pollinations. Next, we examined the *A. thaliana SCRb-SRKb-ARC1* transgenic plants to determine if self-incompatible pollinations resulted in a similar cellular response at the ultrastructural level.

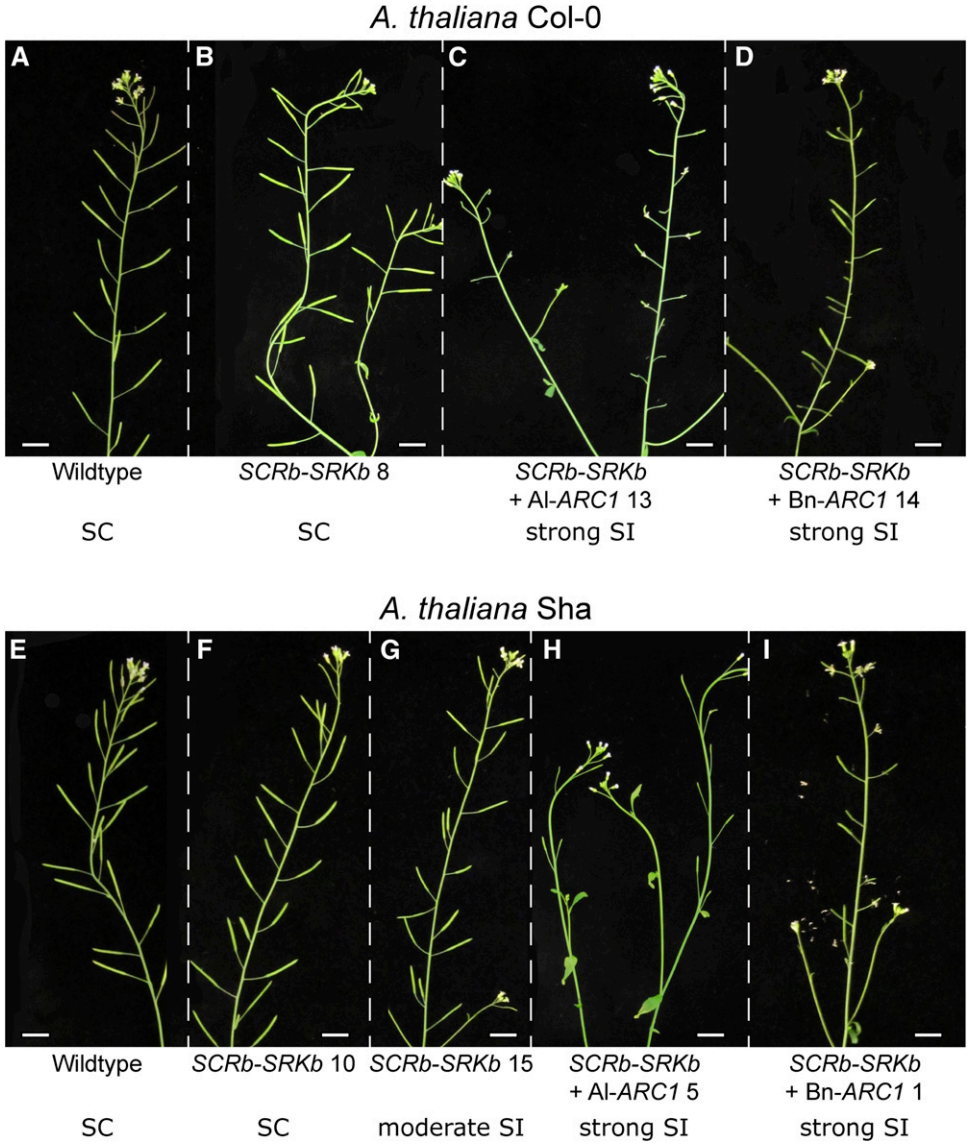

Figure 4. Silique Development in Transgenic *A. thaliana* Col-0 and Sha Plants following Natural Self-Pollination.

(A) and **(E)** Wild-type *A. thaliana* Col-0 and Sha branches with full-sized siliques.
(B) to **(D)** Branches with siliques from *A. thaliana* Col-0 transgenic plants: *SCRb-SRKb* #8, *SCRb-SRKb* + Al-*ARC1* #13, and *SCRb-SRKb* + Bn-*ARC1* #14.
(F) to **(I)** Branches with siliques from *A. thaliana* Sha transgenic plants: *SCRb-SRKb* #10 and 15, *SCRb-SRKb* + Al-*ARC1* #5, and *SCRb-SRKb* + Bn-*ARC1* #1.
SC, self-compatible; SI, self-incompatible. Bars = 1 cm.
[See online article for color version of this figure.]

To enable comparisons with the previous *A. thaliana* Col-0 and *A. lyrata* results (Safavian and Goring, 2013), self-pollinations at 10 min postpollination were examined in the *A. thaliana* Col-0 *SCRb-SRKb* + Al-*ARC1* line 13 (Figure 8) and *A. thaliana* Col-0 *SCRb-SRKb* + Bn-*ARC1* line 8 (Supplemental Figure 4 and Supplemental Table 1). When compared with *A. lyrata* self-incompatible pollinations at 10 min postpollination, there were three observations that were indicative of a conserved ultrastructural self-incompatible response. First, the cytoplasm was clearly visible in all the samples and not compressed by the vacuole under the pollen contact site (Table 4, Figure 8). Second, vesicle-like structures were present in the cytoplasm and not observed fusing to the plasma membrane (Figures 8C and 8D). Finally, in several samples, autophagy appeared to be underway as autophagic bodies were present in the vacuole for degradation (Table 4). The autophagic bodies shown in Figure 8E are similar in appearance to those detected in *A. lyrata* (Figure 7E; Safavian and Goring, 2013). Additionally, multivesicular bodies (MVBs) were observed in the cytoplasm (Figure 8G),

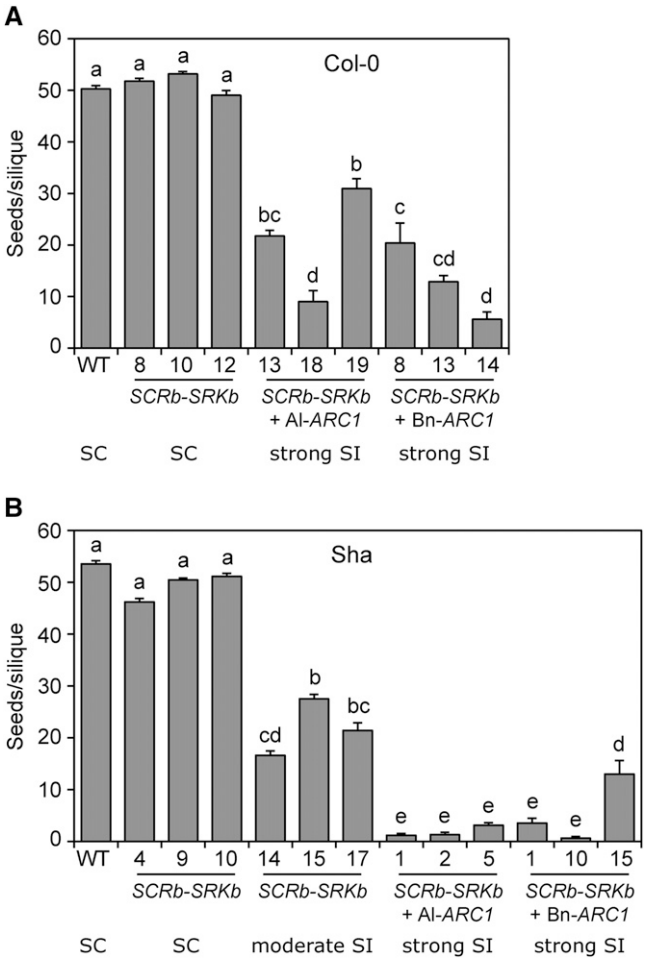

Figure 5. Seed Set in Manually Self-Pollinated Transgenic *A. thaliana* Col-0 and Sha Lines.

(A) Mean seeds/silique for wild-type *A. thaliana* Col-0 and transgenic Col-0 lines following manual self-pollinations. The different letters represent means that are significantly different at $P < 0.001$ (one-way ANOVA with Tukey-HSD post-hoc tests). $n = 30$ siliques.
(B) Mean seeds/silique for wild-type *A. thaliana* Sha and transgenic Sha lines following manual self-pollinations. The different letters represent means that are significantly different at $P < 0.0001$ (one-way ANOVA with Tukey-HSD post-hoc tests). $n = 30$ siliques except for the three moderate self-incompatible Sha *SCRb-SRKb* lines where $n = 10$.
Error bars indicate SE. SC, self-compatible; SI, self-incompatible.

possibly destined to the vacuole for degradation (reviewed in Ding et al., 2012). Interestingly, autophagosomes were observed in the cytoplasm (Figure 8H), which were not previously captured with the rapid responses following *A. lyrata* self-incompatible pollinations (Safavian and Goring, 2013). Similar observations were seen with *A. thaliana* Col-0 *SCRb-SRKb* + Bn-*ARC1* line 8 (Supplemental Figure 4). There were several unexpected observations that we had not previously observed for pollinations in the *Arabidopsis* species. We detected exocyst-positive organelle (EXPO)-like structures (Figure 8F), which have been proposed to be novel transport organelles for protein secretion (Wang et al., 2010; reviewed in Ding et al., 2012). MVBs (Figure 8G) and possibly an autophagosome (Supplemental Figure 4) were observed fusing to the plasma membrane, perhaps escaping degradation in the vacuole and leading to the delivery of factors for pollen hydration. A likely explanation for these results is that the targeting of these structures to the vacuole is impaired and misdirected in these in the transgenic *A. thaliana* Col-0 stigmatic papillae.

To determine if absence or presence of *ARC1* resulted in different ultrastructural features accompanying pollen rejection, we examined the moderately self-incompatible *A. thaliana* Sha *SCRb-SRKb* line 14 and the strongly self-incompatible *A. thaliana* Sha *SCRb-SRKb* + Al-*ARC1* line 2 (Table 4, Figure 9). In both lines, the cytoplasm was clearly visible in the samples and vesicles accumulated in the cytoplasm (Figures 9B to 9H, Table 4), indicating that vesicle secretion is disrupted in the pollen rejection response, regardless of whether ARC1 is present. Vesicle-like structures were observed at the plasma membrane in several of the samples, and these structures may perhaps be responsible for the increased pollen acceptance in these lines (Figures 9B and 9H, Table 4). A MVB fusing to the plasma membrane was only observed in one sample for *A. thaliana* Sha *SCRb-SRKb* line 14 (Table 4). Overall, the targeting of MVBs/autophagosomes to the vacuole at the ultrastructural level in the Sha ecotype (Table 4) was more similar to that observed in *A. lyrata* (Safavian and Goring, 2013) and may contribute to the stronger self-incompatibility phenotype in the Sha ecotype versus the Col-0 ecotype.

One difference observed between *A. thaliana* Sha *SCRb-SRKb* line 14 and *SCRb-SRKb* + Al-*ARC1* line 2 was the presence of autophagic structures in the vacuole. In the *A. thaliana* Sha *SCRb-SRKb* line 14, some cellular debris was present in the vacuoles, but autophagic organelles were not detected (Figure 9C, Table 4). In contrast, *A. thaliana* Sha *SCRb-SRKb* + Al-*ARC1* line 2 contained potential autophagic organelles in the vacuole in 90% of the samples studied (Figures 9E and 9F, Table 4). These autophagic organelles (membrane enclosed structures) are similar in appearance to the Class 2 and Class 3 autophagic vacuoles described by Rose et al. (2006) where the contents are in the process of being digested. Interestingly, in one *A. thaliana* Sha *SCRb-SRKb* line 14 sample, we observed what appears to be an autophagic vacuole in the cytoplasm (Figure 9C), while another sample had both an MVB and a potential phagophore engulfing the cytoplasm (Figure 9D) in the process of forming an autophagosome (reviewed in Yoshimoto, 2012). This suggests that organelles for the degradation of cytoplasmic material can form in the absence of ARC1 but were detected at a low frequency. Therefore, the addition of ARC1 appears to promote autophagy in the *A. thaliana* Sha self-incompatibility response, and this may be responsible for the stronger pollen rejection phenotype observed when *ARC1* is added with *SCRb-SRKb* in the Sha ecotype.

DISCUSSION

Previously, we have shown that the *ARC1* E3 ubiquitin ligase gene is required for Brassicaceae self-incompatibility through knockdown transgenic studies in *B. napus* and *A. lyrata* (Stone et al., 1999; Indriolo et al., 2012). *A. thaliana* is an excellent model system for investigating factors required for restoring self-incompatibility

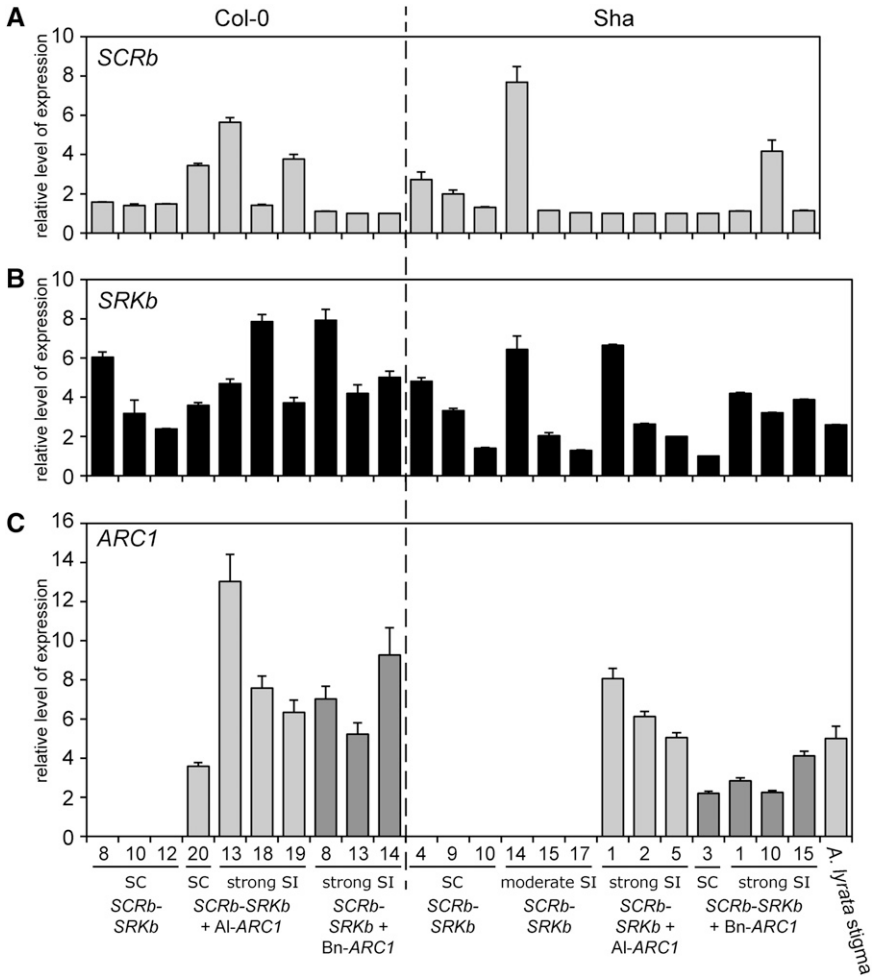

Figure 6. qRT-PCR Analyses of *SCRb*, *SRKb*, and *ARC1* Expression in *A. thaliana* Col-0 and Sha Transgenic Lines.

(A) Relative levels of *SCRb* expression in mature anthers from the different genotypes.

(B) Relative levels of *SRKb* expression in the upper half of mature pistils from the different genotypes.

(C) Relative levels of ARC1expression in the *SCRb-SRKb* + *Al-ARC1* (light gray) or *SCRb-SRKb* + *Bn-ARC1* (dark gray) lines.

The relative levels of *SCRb*, *SRKb*, and *ARC1* expression were normalized to the expression of two control genes, *Elf1*α and *TUB4*. An *A. lyrata* stigma RNA sample was included as a positive control for the relative levels of wild-type Al-*SRK1* and Al-*ARC1*. Means from six technical replicates are shown. Error bars indicate SE. SC, self-compatible; SI, self-incompatible.

as most ecotypes carry pseudogenes for both *SCR* and *SRK* (Kusaba et al., 2001; Bechsgaard et al., 2006; Tang et al., 2007; Shimizu et al., 2008; Boggs et al., 2009a; Tsuchimatsu et al., 2010; Guo et al., 2011), and *ARC1* has been deleted (Kitashiba et al., 2011; Indriolo et al., 2012). Previous studies on the restoration of self-incompatibility in *A. thaliana* with functional *SCR* and *SRK* produced varying results with some ecotypes remaining fully self-compatible, while other ecotypes displayed varying degrees of the self-incompatibility phenotype, but the self-pollen rejection response was incomplete and still produced some seeds (Nasrallah et al., 2004; Boggs et al., 2009a; Tsuchimatsu et al., 2010). We observed that naturally self-incompatible *A. lyrata* ssp *petraea* has a robust self-incompatibility response and produces no seeds, even with manual pollinations to bypass the approach herkogamous and dichogamous traits (Indriolo et al., 2012).

Here in this gain-of-function study, we have shown that *ARC1* is a critical component in reconstituting the self-incompatibility signaling pathway in self-compatible *A. thaliana*, by conferring a stronger and more stable rejection of self-pollen in both the *A. thaliana* Col-0 and Sha ecotypes. Our results for the *A. thaliana* Col-0 ecotype clearly show that the *SCRb-SRKb* construct is not sufficient to produce any self-pollen rejection in fully opened flowers. However, the addition of *ARC1* with *SCRb-SRKb* produced a self-incompatibility phenotype in *A. thaliana* Col-0 that had not been reported in other studies (Nasrallah et al., 2002, 2004; Boggs et al., 2009a). Also, in the *A. thaliana* Sha ecotype, the addition of *ARC1* with *SCRb-SRKb* produced a more robust self-incompatibility response, and for our strongest lines, 60 to 80% of the siliques contained no seeds following manual pollinations. Furthermore, at the ultrastructural level, there were

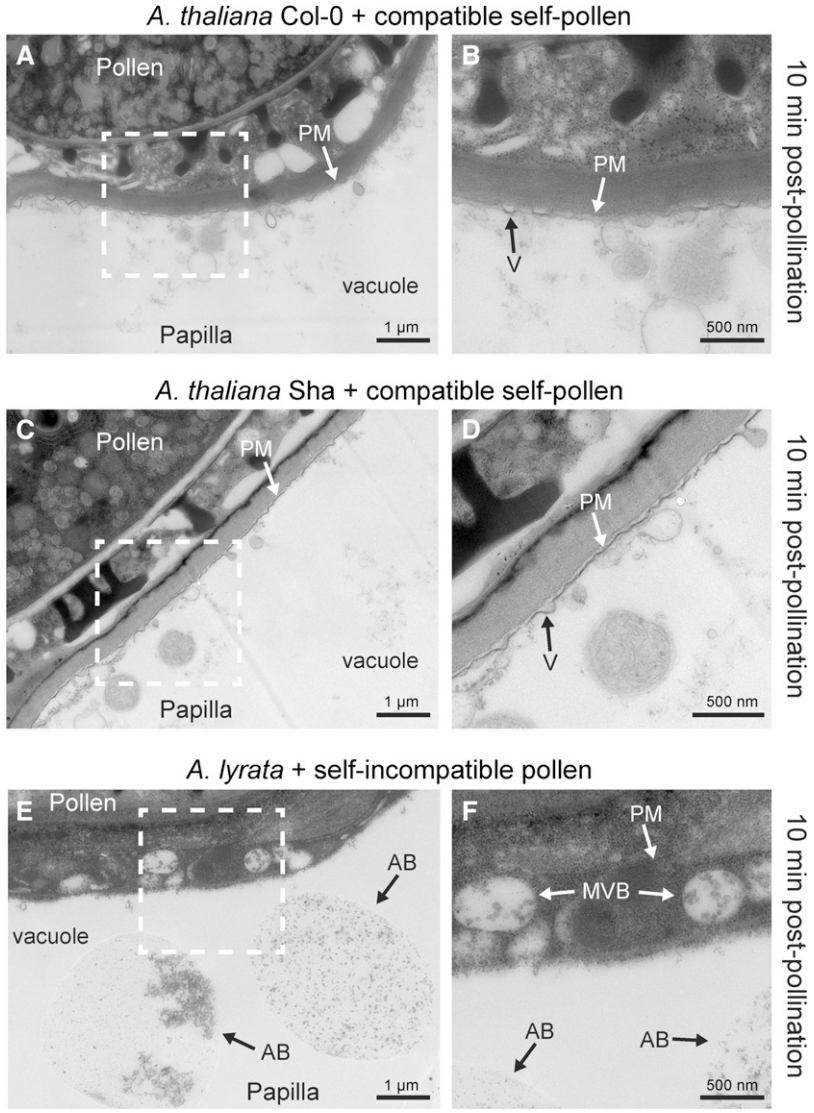

Figure 7. TEM Images of *A. thaliana* Col-0, *A. thaliana* Sha, and *A. lyrata* Stigmatic Papillae in Response to Self-Pollen.

(A) and **(B)** *A. thaliana* Col-0 stigmatic papilla at 10 min postpollination with compatible self-pollen. Vesicles (V) fuse to the plasma membrane (PM) underneath the pollen contact site.

(C) and **(D)** *A. thaliana* Col-0 stigmatic papilla at 10 min postpollination with compatible self-pollen. Vesicles fuse to the plasma membrane underneath the pollen contact site.

(E) and **(F)** *A. lyrata* stigmatic papilla at 10 min postpollination with self-incompatible pollen. Secretory activity was not observed at the papillar plasma membrane. Structures that may represent autophagic bodies (AB) are present in the vacuole. MVBs are present in the cytoplasm, possibly destined to the vacuole.

The white boxed areas in **(A)**, **(C)**, and **(E)** are enlarged in the **(B)**, **(D)**, and **(F)**, respectively. Bars = 1 µm in **(A)**, **(C)**, and **(E)** and 500 nm **(B)**, **(D)**, and **(F)**.

disruptions in vesicle secretion and signs of autophagy as predicted from our previous work (Samuel et al., 2009; Safavian and Goring, 2013). Thus, despite the divergence of the *Brassica* species ~20 to 40 million years ago from the *Arabidopsis* species (Franzke et al., 2011), our study shows that *SCR-SRK-ARC1* signaling is conserved at the cellular level (Figure 10).

It is important to highlight that self-incompatibility is driven by the prevention of the basal compatible pollen response. In the model for the acceptance of a compatible pollen grain, secretory vesicles are tethered under the pollen contact site by Exo70A1 (as part of the exocyst complex), followed by vesicle fusion and the delivery of unknown factors for pollen grain hydration and pollen tube entry (Figure 10A). In the model for the SCRb-SRKb-ARC1 self-incompatibility pathway, the basal pollen response is blocked through Exo70A1 ubiquitination and the induction of autophagy resulting in the removal of secretory vesicles from the pollen contact site by degradation in the vacuole (Figures 10B and 10C). Thus, the presence of ARC1 with SCRb-SRKb inhibits

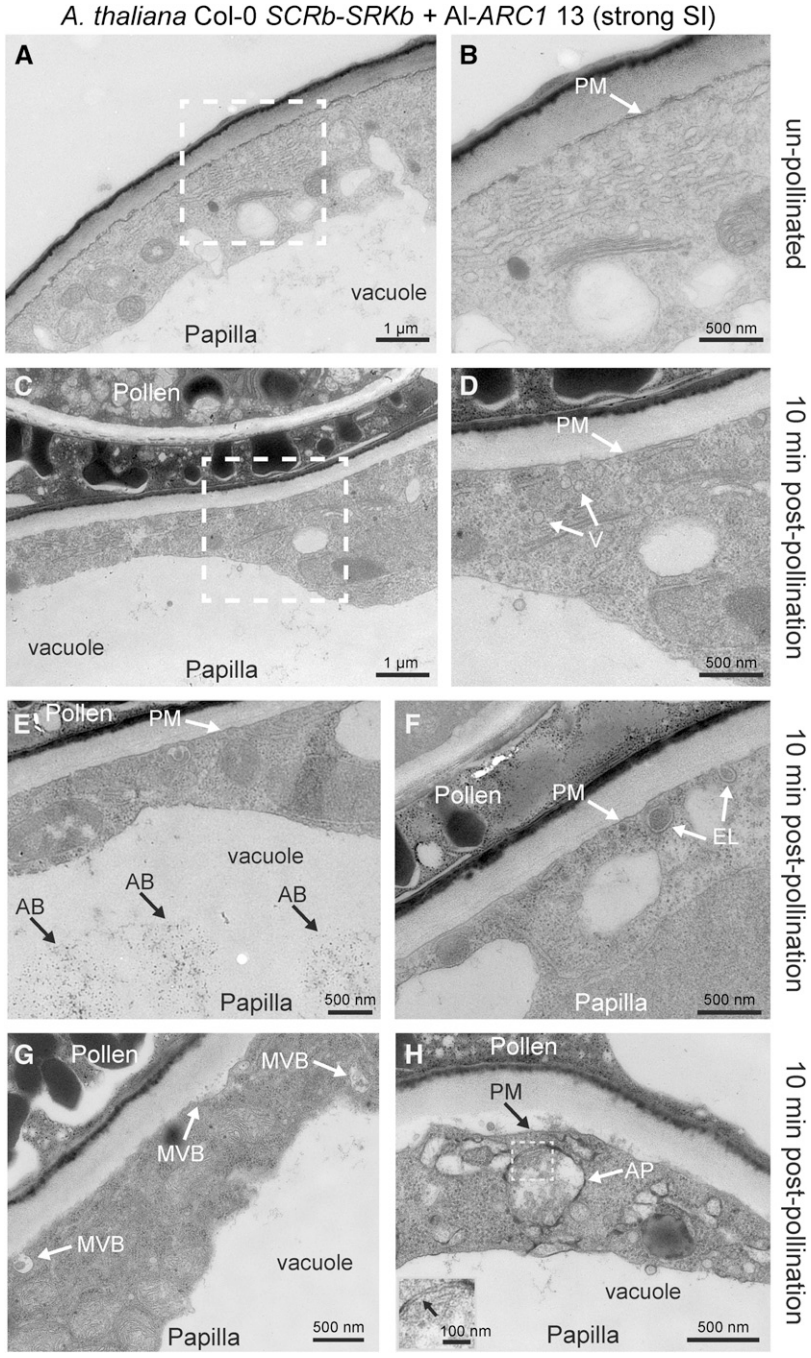

Figure 8. TEM Images of *A. thaliana* Col-0 *SCRb-SRKb* + AI-*ARC1* Line #13 Stigmatic Papillae in Response to Self-Pollen.

(A) and **(B)** Unpollinated stigmatic papilla.
(C) to **(H)** Stigmatic papillae at 10 min postpollination. Several different structures were observed (Table 4), including vesicles (V) in the cytoplasm **(D)**, autophagic bodies (AB) in the vacuole **(E)**, EXPO-like (EL) structures fusing to the plasma membrane (PM) **(F)**, and autophagosomes (A) in the cytoplasm **(H)**. The gray boxed area in **(H)** shows the double membrane of the autophagosome and is displayed in the inset in the bottom left hand corner.
The white boxed areas in **(A)** and **(C)** are shown in **(B)** and **(D)**, respectively. Bars = 1 µm in **(A)** and **(C)** and 500 nm in **(B)** and **(D)** to **(H)**. Bar in **(H)** inset = 100 nm.

Table 4. Cellular Responses in Transgenic *A. thaliana* Plants at 10 min Postpollination

Transgenic Line	Vesicles at PM	Compressed Cytoplasm	EXPO-Like at PM	Autophagosome/ MVBs at PM	Vesicles in Cytoplasm	Autophagosome/ MVBs in Cytoplasm	Debris in Vacuole	Autophagic Organelles in Vacuole	Vesicles in Vacuole
A. thaliana Col-0 *SCRb-SRKb* + Al-*ARC1*-13 strong self-incompatible	0	0	4	6	10	4	7	3	3
A. thaliana Sha *SCRb-SRKb*-14 moderate self-incompatible	6	0	1	1	9	1	6	0	1
A. thaliana Sha *SCRb-SRKb* + Al-*ARC1*-2 strong self-incompatible	5	1	3	0	9	5	5	9	0

Numbers indicate the number of samples. $n = 10$ for each line (where two stigmatic papillae per stigma for five stigmas were examined).

exocytosis at the pollen contact site as observed from the ultrastructural data (Table 4, Figure 9). There is also a correlation between the presence of ARC1 with SCRb-SRKb and autophagy, but we do not know how ARC1 is connected with the induction of autophagy.

When the self-incompatibility response is examined in transgenic *A. thaliana*, it is clear that there is a difference at the cellular level in this response between the Sha and Col-0 ecotypes. Rea et al. (2010) proposed that there are other signaling factors functioning downstream of SRK (Figure 10B). The *A. thaliana* Sha ecotype can reject some self-pollen with *SCRb-SRKb* alone in fully opened flowers (this study; Boggs et al., 2009a). This observation suggests that there is an intrinsic property in the *A. thaliana* Sha ecotype that allows for another unknown signaling pathway(s) downstream of SRK in the pollen rejection response, in addition to the role for ARC1 established in this study (Figure 10B). This alternate signaling pathway(s) appears to be missing or attenuated in the *A. thaliana* Col-0 ecotype as the expression of the *SCRb* and *SRKb* transgenes are at comparable levels to that observed in the transgenic *A. thaliana* Sha *SCRb-SRKb* lines and were unable to solicit any rejection response in fully opened flowers (Figure 10C).

The downstream components of this proposed alternate signaling pathway are unknown, but they appear to function in the prevention of vesicle secretion at the plasma membrane, as we observed an accumulation of vesicles in the cytoplasm. Based on the similarities in this cellular response to what was observed when ARC1 is present, the question arises of whether another PUB protein in the *A. thaliana* Sha ecotype is participating in the SRK signaling pathway. There are 17 *A. thaliana PUB* genes predicted to have the same domain organization as ARC1 (Mudgil et al., 2004). Several of these *PUB* genes are expressed in the stigma (Swanson et al., 2005; Toufighi et al., 2005) and could be candidates for further examination. Another question arising from this work is in regards to the mistrafficking of MVBs and autophagosomes that are observed in the *A. thaliana* Col-0 *SCRb-SRKb* + *ARC1* lines and whether another signaling component in this pathway is differentially regulated in *A. thaliana* Col-0 versus *A. thaliana* Sha. We observed differences in cellular trafficking that may be contributing to the phenotypic variation seen in *A. thaliana* ecotypes expressing *SCRb-SRKb*, and it is likely these differences will contribute to other variable phenotypes across the range of ecotypes studied.

An unexpected and novel result discovered in this study was the development of approach herkogamous flowers with the expression of *ARC1* (with *SRKb*) in *A. thaliana*. This floral morphology trait avoids the deposition of self-pollen on the stigmatic surface and frequently occurs in self-incompatible species (Webb and Lloyd, 1986). These results implicate ARC1 as an important component in driving outcrossing through two distinct mechanisms. The restoration of self-incompatibility and approach herkogamy are fundamental aspects of the biology of an outcrosser and likely the ancestral state of *A. thaliana*. The closely related outcrossing species, *A. lyrata*, is an excellent comparator to *A. thaliana* and has both a functional self-incompatibility system as well as the flower morphology exhibiting approach herkogamy. Recently, two studies on the transition from self-incompatibility to selfing in the genus *Capsella* used QTL analysis to determine the genomic regions that regulate a number of traits in an F2 population from the selfing *C. rubella* crossed with the outcrossing *C. grandiflora*, including the aforementioned self-pollen avoidance traits (Sicard et al., 2011; Slotte et al., 2012). Despite *A. thaliana* typically having non-herkogamous flowers, two *A. thaliana* ecotypes, BRA and SIM, were recently discovered at high altitudes to have approach herkogamous flowers, similar to *A. lyrata*, and a QTL analysis was conducted to map this trait (Luo and Widmer, 2013). QTLs for these traits were described in all of these papers; however, no candidate genes were reported (Sicard et al., 2011; Slotte et al., 2012; Luo and Widmer, 2013). In this study, the approach herkogamous phenotype in wild-type *A thaliana* was only observed when *ARC1* was expressed with the *SCRb-SRKb* construct, suggesting that *SRKb* with *ARC1* is required for this trait. Interestingly, *SRKb* was previously found to cause a stigma exertion phenotype when expressed in the *Arabidopsis* mutant for the RNA-dependent RNA polymerase-6 (*rdr6*) (Tantikanjana et al., 2009). However, we do not know if the approach herkogamy phenotype that we observed in wild-type *A. thaliana* expressing *ARC1* with *SCRb-SRKb* results from a related mechanism to that seen for the stigma exertion phenotype

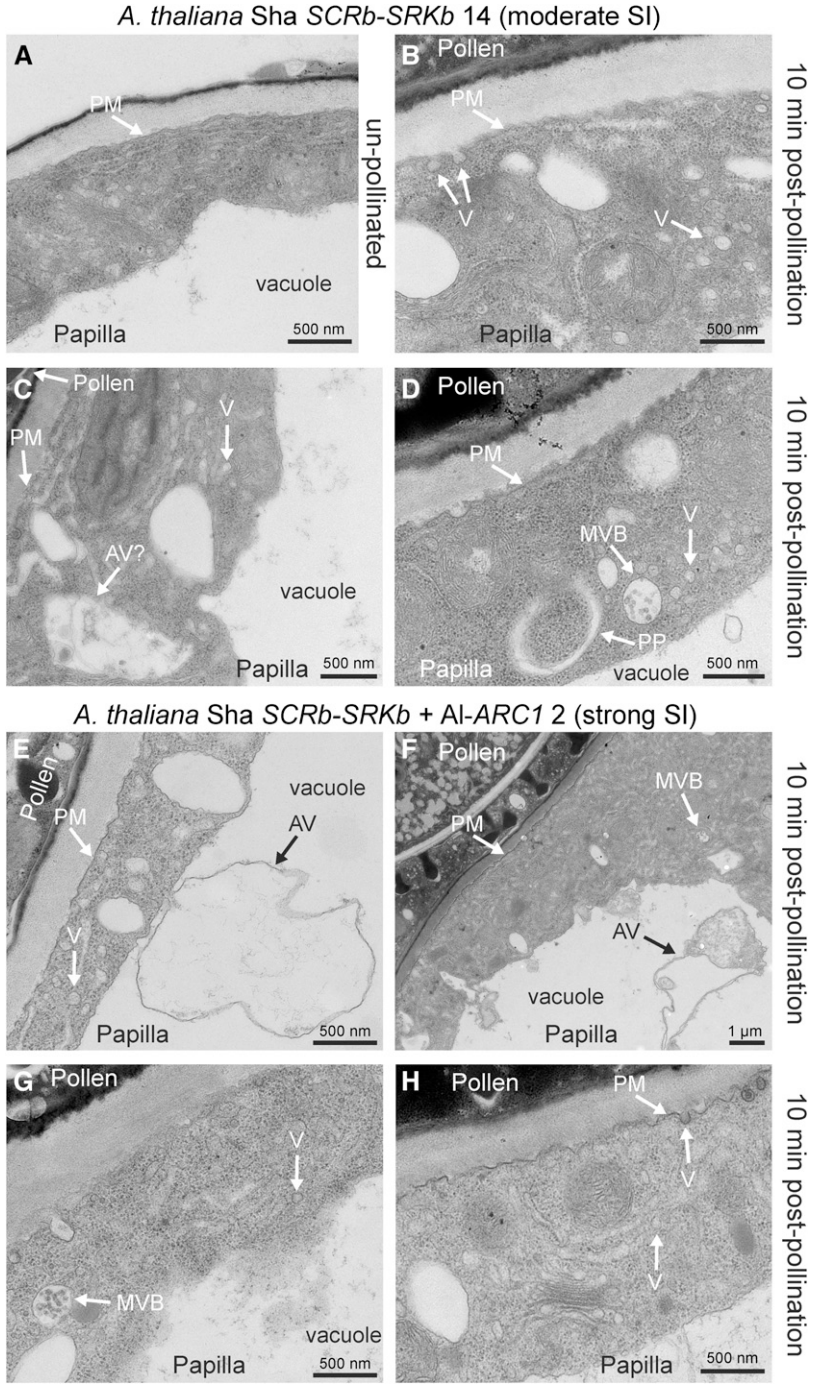

Figure 9. TEM Images of *A. thaliana* Sha *SCRb-SRKb* Line #14 and *A. thaliana* Sha *SCRb-SRKb* + Al-*ARC1* Line #2 Stigmatic Papillae in Response to Self-Pollen.

(A) to **(D)** *A. thaliana* Sha *SCRb-SRKb* line #14 showing unpollinated stigmatic papilla in **(A)** and stigmatic papillae at 10 min postpollination in **(B)** to **(D)**. Several different structures were observed (Table 4) with the main observations being vesicles (V) at the plasma membrane **(B)** or accumulating in the cytoplasm (**[B]** to **[D]**). We also observed a MVB at the plasma membrane **(C)** or in the cytoplasm **(D)** and a structure that appears to be a developing autophagosome (phagophore [PP]) in the cytoplasm **(D)**.

(E) to **(H)** *A. thaliana* Sha *SCRb-SRKb* + Al-*ARC1* line #2 stigmatic papillae at 10 min postpollination. Several different structures were observed (Table 4) with the main observations being vesicles (V) accumulating in the cytoplasm (**[E]** to **[H]**) and autophagic vacuoles (AV) in the vacuole (**[E]** and **[F]**). We also observed MVBs in the cytoplasm **(G)** and vesicles at the plasma membrane **(H)**.

Bars = 1 μm in **(C)** and **(F)** and 500 nm in **(A)**, **(B)**, **(D)**, **(E)**, **(G)**, and **(H)**.

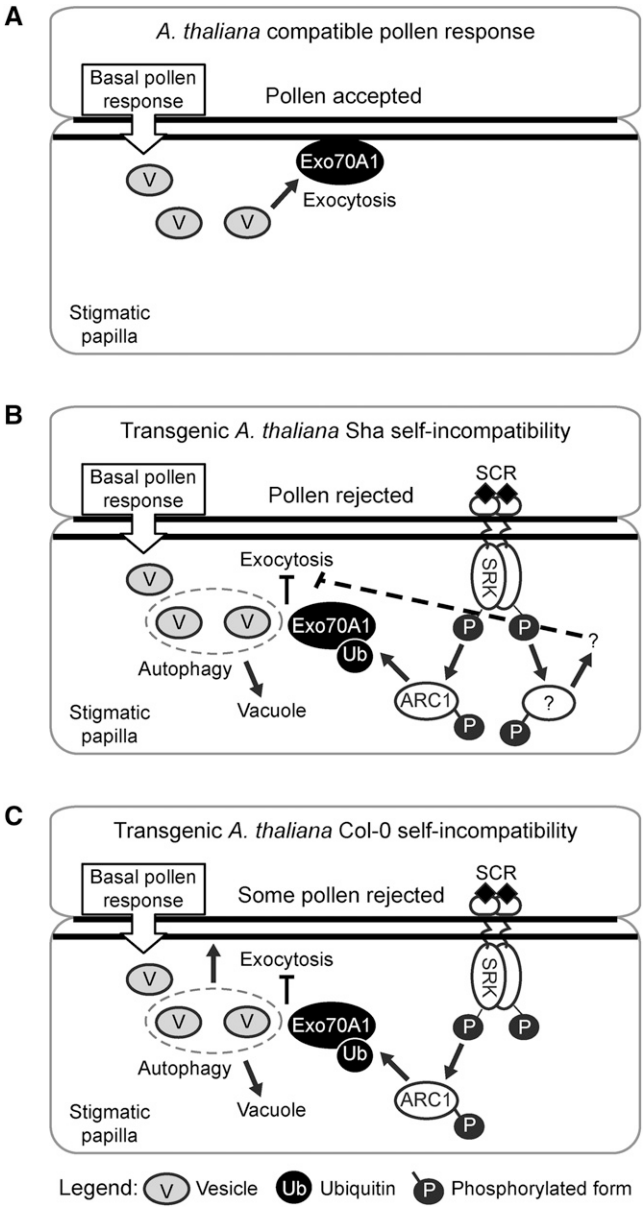

Figure 10. Models of the Reconstituted Self-Incompatibility Signaling Pathways in the Transgenic *A. thaliana* Col-0 and Sha Ecotypes.

(A) In *A. thaliana*, the basal pollen recognition response in the stigmatic papilla leads to activation of vesicle secretion and Exo70A1 is necessary for this (Samuel et al., 2009; Safavian and Goring, 2013).

(B) With self-pollination in the transgenic *A. thaliana* Sha lines, the binding of the pollen SCR ligand to the stigma SRK results in the activation of the self-pollen rejection pathway in the stigmatic papilla. SRK recruits ARC1, and ARC1 then targets Exo70A1 for ubiquitination. Ubiquitinated Exo70A1 is inhibited in its function in directed vesicle secretion (exocytosis), and exocytosis is blocked under the point of pollen contact; as a result, secretory vesicles are sent to the vacuole for degradation via autophagy (Safavian and Goring, 2013). Some pollen rejection can occur when only *SCRb* and *SRKb* are expressed (i.e., no *ARC1*) in the *A. thaliana* Sha ecotype, suggesting that an additional pathway downstream of SRK (?) may be activated to promote pollen rejection. This pathway appears to block exocytosis as vesicles were found to accumulate in the stigmatic papillar cytoplasm for these lines.

(C) With self-pollination in the transgenic *A. thaliana* Col-0 lines, there is one key pathway downstream of SRK, as when only *SCRb* and *SRKb* are expressed (i.e., no *ARC1*), pollen rejection does not occur. When *SCRb-SRKb* + *ARC1* are expressed, a self-incompatible response is activated, but it is not as strong as that seen in the *A. thaliana* Sha ecotype, suggesting that another signaling step downstream of SRK is missing or has reduced activity. Perhaps the unknown factor has a role in the trafficking of MVBs and autophagosomes to the vacuole as this step appears to be impaired in the Col-0 transgenic plants.

resulting from *SRKb* expression in the mutant *rdr6* background (Tantikanjana et al., 2009).

In conclusion, we determined that *ARC1 is* the third component that is required to return *A. thaliana* to its ancestral self-incompatibility state. The observation that *A. lyrata* and *B. napus* ARC1 orthologs performed the same function in this system lends further support to the conserved role of ARC1 in the Brassicaceae self-incompatibility response. Also, we uncovered a role for ARC1 is promoting approach herkogamy as a pollen-avoidance strategy. This observation leads to more questions in regards to what drives the underlying mechanism through which ARC1 can illicit this morphological change in the flower. It would be interesting to determine what other proteins ARC1 regulates through ubiquitination in the context of flower development and self-incompatibility. As both self-incompatibility and approach herkogamy contribute to the ability of a species of the Brassicaceae to be a vigorous outcrosser, this study makes important contributions to our understanding of the molecular mechanisms that contribute to outcrossing when compared with selfing in these economically important plants.

METHODS

Plant Material

The *Arabidopsis thaliana* ecotypes used in this study were from the Col-0 ecotype (CS22625) and Sha (CS22652) both obtained from the Nordborg collection (96 ecotype set; Nordborg et al., 2005) from the ABRC stock center. The self-incompatible perennial *Arabidopsis lyrata* ssp *petraea* plants were previously described (Indriolo et al., 2012). *Arabidopsis* plants were grown in growth chambers under long-day conditions with a 16-h-light/8-h-dark photoperiod at 22°C.

Plant Transformation Vectors

The p548 plant transformation vector that carries the *A. lyrata SCRb* and *SRKb* genes driven under their native promoters was provided by June Nasrallah (Nasrallah et al., 2004; Boggs et al., 2009a). Full-length AlI-*ARC1* was cloned from *A. lyrata* ssp *petraea* genomic DNA using PCR to amplify 5′ and 3′ segments that contain an overlapping region in the middle of the full-length sequence. A 5′ region of the 1.12-kb region and 3′ region of the 1.38-kb fragment were amplified. Then, two fragments were joined using the *Bam*HI site in the middle of AlI-*ARC1* to produce a full-length AlI-*ARC1* clone. The full-length AlI-*ARC1* clone was then amplified with forward and reverse primers with *Xma*I and *Eco*RI sites for directional cloning into the pORE3 binary vector with the SLR1 promoter (Franklin et al., 1996; Indriolo et al., 2012). The SLR1 promoter displays stigma-specific expression in *Arabidopsis* (Foster et al., 2005; Fobis-Loisy et al., 2007). The

Bn-*ARC1* clone (Stone et al., 2003) was amplified with the forward and reverse primers to clone into the *Xma*I site of the p1665 plant transformation vector with the SLR1 promoter (Samuel et al., 2009). See Supplemental Table 2 for PCR primers used in these cloning steps. All PCR products were amplified with Advantage 2 polymerase (Clontech), subcloned into pGEMTeasy (Promega), and verified by sequencing before proceeding to the next step. The transformation vectors were electroporated into *Agrobacterium tumefaciens*, and successful transformants were verified by PCR.

Plant Transformation

A. thaliana plants were transformed by the floral dip method (Clough and Bent, 1998), and multiple constructs were transformed as previously described (Davis et al., 2009). Seeds from dipped plants were collected and screened for resistance by spraying seedlings with 0.1% Basta or plating seeds on half-strength Murashige and Skoog plates with 50 μg/mL kanamycin. For screening double transformation events (p548 plant transformation vector and the ARC1 transformation vector), selections were only performed for one resistance marker to avoid stressing the plants and survivors were then genotyped by PCR for both constructs. Self-incompatible transgenic T2 plants were confirmed to carry both the *SCRb-SRKb* and *ARC1* constructs by PCR genotyping (Supplemental Figure 5).

PCR Assays

For the qRT-PCR assays, RNA was extracted from 1/2 pistils (stigma and style) and mature anthers, and cDNA synthesis was performed as previously described (Indriolo et al., 2012).

The qRT-PCR was performed as previously described (Indriolo et al., 2012) using either pistil cDNA or anther cDNA and 2× KAPA SYBR FAST Master Mix (KAPA). Following the qRT-PCR reactions, the *SCRb*, *SRKb*, Al-*ARC1*, and Bn-*ARC1* expression levels were normalized to two controls, *Elf1a* and *TUB4*. Tsg polymerase (Biobasics) was used for all the PCR reactions, and the conditions used were a 3-min denaturation at 95°C, followed by a two-step cycle of 3 s 95°C denaturation, 20 s at the appropriate annealing temperature, and extension for 40 cycles with a melt curve. See Supplemental Table 2 for the list of qRT-PCR primers used in this study.

Crosses and Pollination Assays

All crosses on the *A. thaliana* Col-0 and Sha transgenic plants were performed at the stage where the flowers are fully opened. Stage 12 buds (Smyth et al., 1990) were emasculated, covered in plastic wrap, and left for 24 h prior to manual pollination. For the aniline blue staining, manually pollinated pistils were left for 2 h followed by fixing and staining as previously described (Samuel et al., 2009). For seed set analysis, the manually pollinated pistils were left to develop into siliques, and once close to shattering, the siliques were dissected and the total number of seeds was tallied. A total of 10 siliques per plant, for three different siblings per independent line were analyzed. For the TEM analysis, pollinations and analyses were performed as previously described (Safavian and Goring, 2013) using a Hitachi HT7700 transmission electron microscope at 75 kV. Silique branch photos were taken with a Canon Cybershot digital camera, and flower photos were taken under a dissecting microscope. For the approach herkogamous phenotype, SAS measurements were taken as previously described by Luo and Widmer (2013).

Accession Numbers

The ARC1 sequence data from *A. lyrata* ssp *petraea* can be found in GenBank under ID KF418158. The SRK1 sequence data from *A. lyrata* ssp *petraea* can be found in GenBank under ID KF418159.

Supplemental Data

The following materials are available in the online version of this article.

Supplemental Figure 1. Alignment of *A. lyrata* ARC1 and *B. napus* ARC1 Amino Acid Sequences.

Supplemental Figure 2. Pollen Grain Attachment and Pollen Tube Growth in Reciprocal Crosses between the Transgenic *A. thaliana* Col-0 and Sha Lines with Wild-Type *A. thaliana* Col-0 and Sha Plants, Respectively.

Supplemental Figure 3. The Approach Herkogamy Phenotype Arises from Increased Pistil Length in the *A. thaliana SCRb-SRKb* + *ARC1* Transgenic Flowers.

Supplemental Figure 4. TEM Images of *A. thaliana* Sha *SCRb-SRKb* Line 14 and *A. thaliana* Sha *SCRb-SRKb* + Al-*ARC1* Line 2 Stigmatic Papillae in Response to Self-Pollen.

Supplemental Figure 5. Genotypes of Self-Incompatible Transgenic T2 Progeny.

Supplemental Table 1. Cellular Responses in Transgenic *A. thaliana* Plants at 10 min Postpollination.

Supplemental Table 2. Primers Used for PCR Cloning and Analyses.

ACKNOWLEDGMENTS

We thank June Nasrallah for providing the p548 transformation vector with the *A. lyrata SRKb* and *SCRb* genes and Audrey Darabie of the Cell and Systems Biology Imaging facility for assistance with the TEM. D.S. is supported by an Ontario Graduate Scholarship, and this research was supported by grants from Natural Sciences and Engineering Research Council of Canada and a Canada Research Chair to D.R.G.

AUTHOR CONTRIBUTIONS

E.I. designed the research, performed research, analyzed data, and wrote the article. D.S. designed the research, performed research, and analyzed data. D.R.G. designed the research, analyzed data, and wrote the article.

Received January 10, 2014; revised March 19, 2014; accepted March 27, 2014; published April 18, 2014.

REFERENCES

Barrett, S.C. (2003). Mating strategies in flowering plants: the outcrossing-selfing paradigm and beyond. Philos. Trans. R. Soc. Lond. B Biol. Sci. **358:** 991–1004.

Bechsgaard, J.S., Castric, V., Charlesworth, D., Vekemans, X., and Schierup, M.H. (2006). The transition to self-compatibility in *Arabidopsis thaliana* and evolution within S-haplotypes over 10 Myr. Mol. Biol. Evol. **23:** 1741–1750.

Boggs, N.A., Dwyer, K.G., Shah, P., McCulloch, A.A., Bechsgaard, J., Schierup, M.H., Nasrallah, M.E., and Nasrallah, J.B. (2009b). Expression of distinct self-incompatibility specificities in *Arabidopsis thaliana*. Genetics **182:** 1313–1321.

Boggs, N.A., Nasrallah, J.B., and Nasrallah, M.E. (2009a). Independent S-locus mutations caused self-fertility in *Arabidopsis thaliana*. PLoS Genet. **5:** e1000426.

Chapman, L.A., and Goring, D.R. (2010). Pollen-pistil interactions regulating successful fertilization in the Brassicaceae. J. Exp. Bot. **61:** 1987–1999.

Charlesworth, D. (2006). Evolution of plant breeding systems. Curr. Biol. **16:** R726–R735.

Clough, S.J., and Bent, A.F. (1998). Floral dip: a simplified method for Agrobacterium-mediated transformation of *Arabidopsis thaliana*. Plant J. **16:** 735–743.

Davis, A.M., Hall, A., Millar, A.J., Darrah, C., and Davis, S.J. (2009). Protocol: Streamlined sub-protocols for floral-dip transformation and selection of transformants in *Arabidopsis thaliana*. Plant Methods **5:** 3.

Ding, Y., Wang, J., Wang, J., Stierhof, Y.D., Robinson, D.G., and Jiang, L. (2012). Unconventional protein secretion. Trends Plant Sci. **17:** 606–615.

Fobis-Loisy, I., Chambrier, P., and Gaude, T. (2007). Genetic transformation of *Arabidopsis lyrata*: specific expression of the green fluorescent protein (GFP) in pistil tissues. Plant Cell Rep. **26:** 745–753.

Foster, E., Levesque-Lemay, M., Schneiderman, D., Albani, D., Schernthaner, J., Routly, E., and Robert, L.S. (2005). Characterization of a gene highly expressed in the *Brassica napus* pistil that encodes a novel proline-rich protein. Sex. Plant Reprod. **17:** 261–267.

Franklin, T.M., Oldknow, J., and Trick, M. (1996). SLR1 function is despensible for both self-incompatible and self-compatible pollination processes in Brassica. Sex. Plant Reprod. **9:** 203–208.

Franzke, A., Lysak, M.A., Al-Shehbaz, I.A., Koch, M.A., and Mummenhoff, K. (2011). Cabbage family affairs: the evolutionary history of Brassicaceae. Trends Plant Sci. **16:** 108–116.

Gu, T., Mazzurco, M., Sulaman, W., Matias, D.D., and Goring, D.R. (1998). Binding of an arm repeat protein to the kinase domain of the S-locus receptor kinase. Proc. Natl. Acad. Sci. USA **95:** 382–387.

Guo, Y.L., Bechsgaard, J.S., Slotte, T., Neuffer, B., Lascoux, M., Weigel, D., and Schierup, M.H. (2009). Recent speciation of *Capsella rubella* from *Capsella grandiflora*, associated with loss of self-incompatibility and an extreme bottleneck. Proc. Natl. Acad. Sci. USA **106:** 5246–5251.

Guo, Y.L., Zhao, X., Lanz, C., and Weigel, D. (2011). Evolution of the S-locus region in Arabidopsis relatives. Plant Physiol. **157:** 937–946.

Hamasaki, M., Noda, T., Baba, M., and Ohsumi, Y. (2005). Starvation triggers the delivery of the endoplasmic reticulum to the vacuole via autophagy in yeast. Traffic **6:** 56–65.

Heider, M.R., and Munson, M. (2012). Exorcising the exocyst complex. Traffic **13:** 898–907.

Indriolo, E., Tharmapalan, P., Wright, S.I., and Goring, D.R. (2012). The ARC1 E3 ligase gene is frequently deleted in self-compatible Brassicaceae species and has a conserved role in *Arabidopsis lyrata* self-pollen rejection. Plant Cell **24:** 4607–4620.

Ivanov, R., Fobis-Loisy, I., and Gaude, T. (2010). When no means no: guide to Brassicaceae self-incompatibility. Trends Plant Sci. **15:** 387–394.

Iwano, M., and Takayama, S. (2012). Self/non-self discrimination in angiosperm self-incompatibility. Curr. Opin. Plant Biol. **15:** 78–83.

Kachroo, A., Schopfer, C.R., Nasrallah, M.E., and Nasrallah, J.B. (2001). Allele-specific receptor-ligand interactions in Brassica self-incompatibility. Science **293:** 1824–1826.

Kakita, M., Murase, K., Iwano, M., Matsumoto, T., Watanabe, M., Shiba, H., Isogai, A., and Takayama, S. (2007b). Two distinct forms of M-locus protein kinase localize to the plasma membrane and interact directly with S-locus receptor kinase to transduce self-incompatibility signaling in *Brassica rapa*. Plant Cell **19:** 3961–3973.

Kakita, M., Shimosato, H., Murase, K., Isogai, A., and Takayama, S. (2007a). Direct interaction between the S-locus receptor kinase and M-locus protein kinase involved in Brassica self-incompatibility signaling. Plant Biotechnol. **24:** 185–190.

Kitashiba, H., Liu, P., Nishio, T., Nasrallah, J.B., and Nasrallah, M.E. (2011). Functional test of Brassica self-incompatibility modifiers in *Arabidopsis thaliana*. Proc. Natl. Acad. Sci. USA **108:** 18173–18178.

Kusaba, M., Dwyer, K., Hendershot, J., Vrebalov, J., Nasrallah, J.B., and Nasrallah, M.E. (2001). Self-incompatibility in the genus Arabidopsis: characterization of the S locus in the outcrossing *A. lyrata* and its autogamous relative *A. thaliana*. Plant Cell **13:** 627–643.

Lloyd, D.G., and Webb, C.J. (1986). The avoidance of interference between the presentation of pollen and stigmas in Angiosperms. I. Dichogamy. N.Z. J. Bot. **24:** 135–162.

Luo, Y., and Widmer, A. (2013). Herkogamy and its effects on mating patterns in *Arabidopsis thaliana.* PLoS ONE **8:** e57902.

Mable, B.K., and Adam, A. (2007). Patterns of genetic diversity in outcrossing and selfing populations of *Arabidopsis lyrata*. Mol. Ecol. **16:** 3565–3580.

Mudgil, Y., Shiu, S.H., Stone, S.L., Salt, J.N., and Goring, D.R. (2004). A large complement of the predicted Arabidopsis ARM repeat proteins are members of the U-box E3 ubiquitin ligase family. Plant Physiol. **134:** 59–66.

Murase, K., Shiba, H., Iwano, M., Che, F.S., Watanabe, M., Isogai, A., and Takayama, S. (2004). A membrane-anchored protein kinase involved in Brassica self-incompatibility signaling. Science **303:** 1516–1519.

Nakatogawa, H., and Ohsumi, Y. (2008). Starved cells eat ribosomes. Nat. Cell Biol. **10:** 505–507.

Nasrallah, M.E., Liu, P., and Nasrallah, J.B. (2002). Generation of self-incompatible *Arabidopsis thaliana* by transfer of two S locus genes from *A. lyrata*. Science **297:** 247–249.

Nasrallah, M.E., Liu, P., Sherman-Broyles, S., Boggs, N.A., and Nasrallah, J.B. (2004). Natural variation in expression of self-incompatibility in *Arabidopsis thaliana*: implications for the evolution of selfing. Proc. Natl. Acad. Sci. USA **101:** 16070–16074.

Nordborg, M., et al. (2005). The pattern of polymorphism in *Arabidopsis thaliana*. PLoS Biol. **3:** e196.

Nordquist, K.A., Dimitrova, Y.N., Brzovic, P.S., Ridenour, W.B., Munro, K.A., Soss, S.E., Caprioli, R.M., Klevit, R.E., and Chazin, W.J. (2010). Structural and functional characterization of the monomeric U-box domain from E4B. Biochemistry **49:** 347–355.

Paetsch, M., Mayland-Quellhorst, S., and Neuffer, B. (2006). Evolution of the self-incompatibility system in the Brassicaceae: identification of S-locus receptor kinase (SRK) in self-incompatible *Capsella grandiflora*. Heredity (Edinb.) **97:** 283–290.

Prigoda, N.L., Nassuth, A., and Mable, B.K. (2005). Phenotypic and genotypic expression of self-incompatibility haplotypes in *Arabidopsis lyrata* suggests unique origin of alleles in different dominance classes. Mol. Biol. Evol. **22:** 1609–1620.

Rea, A.C., Liu, P., and Nasrallah, J.B. (2010). A transgenic self-incompatible *Arabidopsis thaliana* model for evolutionary and mechanistic studies of crucifer self-incompatibility. J. Exp. Bot. **61:** 1897–1906.

Rose, T.L., Bonneau, L., Der, C., Marty-Mazars, D., and Marty, F. (2006). Starvation-induced expression of autophagy-related genes in *Arabidopsis.* Biol. Cell **98:** 53–67.

Safavian, D., and Goring, D.R. (2013). Secretory activity is rapidly induced in stigmatic papillae by compatible pollen, but inhibited for self-incompatible pollen in the Brassicaceae. PLoS ONE **8:** e84286.

Samuel, M.A., Chong, Y.T., Haasen, K.E., Aldea-Brydges, M.G., Stone, S.L., and Goring, D.R. (2009). Cellular pathways regulating responses to compatible and self-incompatible pollen in Brassica and Arabidopsis stigmas intersect at Exo70A1, a putative component of the exocyst complex. Plant Cell **21:** 2655–2671.

Schierup, M.H., Bechsgaard, J.S., Nielsen, L.H., and Christiansen, F.B. (2006). Selection at work in self-incompatible *Arabidopsis lyrata*: mating patterns in a natural population. Genetics **172:** 477–484.

Schierup, M.H., Mable, B.K., Awadalla, P., and Charlesworth, D. (2001). Identification and characterization of a polymorphic receptor kinase gene linked to the self-incompatibility locus of *Arabidopsis lyrata*. Genetics **158:** 387–399.

Shimizu, K.K., Shimizu-Inatsugi, R., Tsuchimatsu, T., and Purugganan, M.D. (2008). Independent origins of self-compatibility in *Arabidopsis thaliana*. Mol. Ecol. **17:** 704–714.

Shimosato, H., Yokota, N., Shiba, H., Iwano, M., Entani, T., Che, F. S., Watanabe, M., Isogai, A., and Takayama, S. (2007). Characterization of the SP11/SCR high-affinity binding site involved in self/nonself recognition in brassica self-incompatibility. Plant Cell **19:** 107–117.

Sicard, A., Stacey, N., Hermann, K., Dessoly, J., Neuffer, B., Bäurle, I., and Lenhard, M. (2011). Genetics, evolution, and adaptive significance of the selfing syndrome in the genus Capsella. Plant Cell **23:** 3156–3171.

Slotte, T., Hazzouri, K.M., Stern, D., Andolfatto, P., and Wright, S.I. (2012). Genetic architecture and adaptive significance of the selfing syndrome in Capsella. Evolution **66:** 1360–1374.

Smyth, D.R., Bowman, J.L., and Meyerowitz, E.M. (1990). Early flower development in *Arabidopsis.* Plant Cell **2:** 755–767.

Stone, S.L., Anderson, E.M., Mullen, R.T., and Goring, D.R. (2003). ARC1 is an E3 ubiquitin ligase and promotes the ubiquitination of proteins during the rejection of self-incompatible Brassica pollen. Plant Cell **15:** 885–898.

Stone, S.L., Arnoldo, M., and Goring, D.R. (1999). A breakdown of Brassica self-incompatibility in ARC1 antisense transgenic plants. Science **286:** 1729–1731.

Swanson, R., Clark, T., and Preuss, D. (2005). Expression profiling of Arabidopsis stigma tissue identifies stigma-specific genes. Sex. Plant Reprod. **18:** 163–171.

Takayama, S., Shimosato, H., Shiba, H., Funato, M., Che, F.S., Watanabe, M., Iwano, M., and Isogai, A. (2001). Direct ligand-receptor complex interaction controls Brassica self-incompatibility. Nature **413:** 534–538.

Tang, C., Toomajian, C., Sherman-Broyles, S., Plagnol, V., Guo, Y.L., Hu, T.T., Clark, R.M., Nasrallah, J.B., Weigel, D., and Nordborg, M. (2007). The evolution of selfing in *Arabidopsis thaliana*. Science **317:** 1070–1072.

Tantikanjana, T., Rizvi, N., Nasrallah, M.E., and Nasrallah, J.B. (2009). A dual role for the S-locus receptor kinase in self-incompatibility and pistil development revealed by an Arabidopsis *rdr6* mutation. Plant Cell **21:** 2642–2654.

Toufighi, K., Brady, S.M., Austin, R., Ly, E., and Provart, N.J. (2005). The Botany Array Resource: e-Northerns, Expression Angling, and promoter analyses. Plant J. **43:** 153–163.

Tsuchimatsu, T., Suwabe, K., Shimizu-Inatsugi, R., Isokawa, S., Pavlidis, P., Städler, T., Suzuki, G., Takayama, S., Watanabe, M., and Shimizu, K.K. (2010). Evolution of self-compatibility in Arabidopsis by a mutation in the male specificity gene. Nature **464:** 1342–1346.

Wang, J., Ding, Y., Wang, J., Hillmer, S., Miao, Y., Lo, S.W., Wang, X., Robinson, D.G., and Jiang, L. (2010). EXPO, an exocyst-positive organelle distinct from multivesicular endosomes and autophagosomes, mediates cytosol to cell wall exocytosis in Arabidopsis and tobacco cells. Plant Cell **22:** 4009–4030.

Webb, C.J., and Lloyd, D.G. (1986). The avoidance of interference between the presentation of pollen and stigmas in Angiosperms. II. Herkogamy. N.Z. J. Bot. **24:** 163–178.

Xu, Z., Kohli, E., Devlin, K.I., Bold, M., Nix, J.C., and Misra, S. (2008). Interactions between the quality control ubiquitin ligase CHIP and ubiquitin conjugating enzymes. BMC Struct. Biol. **8:** 26.

Yoshimoto, K. (2012). Beginning to understand autophagy, an intracellular self-degradation system in plants. Plant Cell Physiol. **53:** 1355–1365.

Zhang, M., Windheim, M., Roe, S.M., Peggie, M., Cohen, P., Prodromou, C., and Pearl, L.H. (2005). Chaperoned ubiquitylation—crystal structures of the CHIP U box E3 ubiquitin ligase and a CHIP-Ubc13-Uev1a complex. Mol. Cell **20:** 525–538.

Zhang, Y., Liu, C.M., Emons, A.M., and Ketelaar, T. (2010). The plant exocyst. J. Integr. Plant Biol. **52:** 138–146.